ARTICLE

Insight into hydraulic conductivity testing of geosynthetic clay liners (GCLs) exhumed after 5 and 7 years in a cover

R.K. Rowe, R.W.I. Brachman, M.S. Hosney, W.A. Take, and D.N. Arnepalli

Abstract: Four geosynthetic clay liners (GCLs) serving as single liners were exhumed from below 0.7 m of silty sand on a 3:1 (horizontal:vertical) north-facing slope at the QUELTS site in Godfrey, Ontario, after 5 and 7 years. The 300 mm GCL overlaps with 0.4 kg/m supplemental bentonite were all physically intact. The exchangeable bound sodium was completely replaced with divalent cations. The GCL with the smallest needle-punched bundle size (average of 0.7 mm) and percentage area covered by bundles (4%) maintained low hydraulic conductivity (k) when tested under 0.07–1.2 m head with 10 mmol/L $CaCl_2$ solution as the permeant. For GCLs with larger bundles (1.1–1.6 mm) and higher percentage area covered by bundles (9%–14%), k was low when the head was low (0.07 m). Once the applied head increased, k increased by 1–4 orders of magnitude depending on the (*i*) hydraulic gradient, (*ii*) size and number of the needle-punched bundles, and (*iii*) structure and mass of the bentonite per unit area. The results suggest that the GCLs can perform effectively as a single hydraulic barrier in covers providing that the head above the GCL is kept low (e.g., by a suitable drainage layer above the GCL).

Key words: geosynthetic clay liner, cover, overlaps, cation exchange, hydraulic conductivity, field study.

Résumé : Quatre couches d'argile géosynthétiques (CAG) agissant comme des parois uniques ont été exhumés d'une profondeur en dessous de 0,7 m sur un sable limoneux de 3 : 1 (horizontale : verticale) au versant nord au site QUELTS dans Godfrey, en Ontario, après 5 et 7 ans. Les 300 mm de CAG se superposent au 0,4 kg/m de bentonite supplémentaire qui est physiquement intact. Le sodium lié échangeable a été complètement remplacé par des cations divalents. Le CAG avec la plus petite taille de paquet aiguilleté (moyenne de 0,7 mm) et le pourcentage de la superficie couverte par des faisceaux (4 %) a maintenu une faible conductivité hydraulique (k) lors de l'essai sous une tête de 0,07 à 1,2 m avec une solution 10 mM de $CaCl_2$ comme perméant. Pour les CAG avec de plus grands faisceaux (1,1 à 1,6 mm) et un pourcentage plus élevé de la zone couverte par des faisceaux (9–14 %), k est faible quand la tête était faible (0,07 m). Une fois que la tête appliquée a augmenté, k a augmenté de 1 à 4 ordres de grandeur en fonction (*i*) du gradient hydraulique, (*ii*) du nombre et de la taille des faisceaux aiguilletés et (*iii*) de la structure et la masse de la bentonite par unité de surface. Les résultats suggèrent que le CAG peut fonctionner efficacement comme une seule barrière hydraulique dans des couvercles à condition que la tête au-dessus du CAG soit maintenue à un niveau bas (p. ex., par une couche de drainage approprié au-dessus du GCL). [Traduit par la Rédaction]

Mots-clés : couche d'argile géosynthétique, couvercle, chevauchements, échange de cations, conductivité hydraulique, étude sur le terrain.

Introduction

Geosynthetic clay liners (GCLs) have become a common replacement for compacted clays in landfill base liners and cover systems because of their very low hydraulic conductivity (k) to water (Rowe et al. 2004), ability to maintain a low k at relatively high strain (Bouazza et al. 1996), high self-healing capacity when hydrated with water not containing significant cations (Didier et al. 2000; Rowe et al. 2008), and relatively easy installation (Bathurst et al. 2006).

Numerous laboratory investigations have examined the effect of several factors on the hydraulic performance of GCLs such as cation exchange, interaction with different permeants, wet–dry cycles, and freeze–thaw cycles (e.g., Shan and Daniel 1991; Boardman and Daniel 1996; Petrov and Rowe 1997; Lin and Benson 2000; Shackelford et al. 2000, 2010; Jo et al. 2005; Lee et al. 2005; Rowe et al. 2006; Bouazza et al. 2007; Brown and Shackelford 2007;

Benson and Meer 2009; Lange et al. 2010; Rosin-Paumier et al. 2011; Rosin-Paumier and Touze-Foltz 2012; Rowe and Abdelatty 2012; Bradshaw et al. 2013, 2016; Mazzieri et al. 2013; Rowe and Hosney 2013; Sari and Chai 2013). There have been far fewer studies examining the hydraulic performance of GCLs after a period of field exposure in applications such as covers or caps under low applied stress and these studies have given rise to some apparently inconsistent findings as discussed below (James et al. 1997; Benson et al. 2007, 2010; Meer and Benson 2007; Scalia and Benson 2010a, 2011; Buckley et al. 2012; Hosney and Rowe 2013).

Melchior (2002) and Melchior et al. (2010) examined water flow through a needle-punched GCL, forming part of a cover, into two lysimeters (100 m² each) at a landfill near Hamburg, Germany. The cover had a gentle (8%) slope and the GCL was covered by a 0.15 m thick drainage layer (1–8 mm gravel) overlain by a 0.30 m thick top soil layer (loamy sand). The use of only 0.45 m overburden above

R.K. Rowe,* R.W.I. Brachman, and W.A. Take.* GeoEngineering Centre at Queen's-RMC, Queen's University, Ellis Hall, Kingston ON K7L 3N6, Canada.
M.S. Hosney. GeoEngineering Centre at Queen's-RMC, Queen's University, Ellis Hall, Kingston ON K7L 3N6, Canada; Faculty of Engineering, Cairo University, Cairo, Egypt (on leave).
D.N. Arnepalli. Department of Civil Engineering, Indian Institute of Technology Madras.
Corresponding author: R.K. Rowe (email: kerry.rowe@queensu.ca).
*R.K. Rowe and W.A. Take currently serve as Associate Editors; peer review and editorial decisions regarding this manuscript were handled by C. Shackelford.

the GCL was intended to accelerate the influence of desiccation and plant root penetration on the GCL performance. The average annual precipitation at the site was 760 mm. Root penetration through the GCL occurred within 5 months of installation and a network of cracks, which did not visually heal after rewetting of the GCL, was developed after 1 year. Despite these conditions, the percolation though the GCL in the first year was ≤6 mm. Four years after installation, the combined effect of the low confining stress (0.45 m of cover soil), cation exchange, and exposure to wet–dry cycles resulted in an increase in the average annual percolation rate into the two lysimeters to 188–222 mm/year. Under a unit hydraulic gradient, the k value of the GCL inferred from these percolation rates is $6–7 \times 10^{-9}$ m/s. The bentonite in GCL samples exhumed from the test cover had changed from sodium to calcium bentonite due to cation exchange, with a reduction in the mole fraction of sodium (ESP) from 69% (virgin) to 4% and the swell index (SI) decreased from 25–30 mL/2 g (virgin) to 8–15 mL/2 g. The k value measured in the laboratory for exhumed GCL samples was between 2×10^{-6} and 1×10^{-7} m/s (the permeant, effective stress, and hydraulic gradient were not reported). Thus, the k values measured in the laboratory were 2–3 orders of magnitude higher than the k values calculated based on the percolation rates; begging the question — why?

Percolation from a final cover over a coal ash landfill located in Wisconsin, USA, was reported by Benson et al. (2007). The cover profile consisted of a needle-punched GCL overlain by a 0.76 m layer of vegetated silty sand and underlain with a two gravel-filled lysimeters (4.3 m × 4.9 m each) installed to monitor percolation. The average annual precipitation was 892 mm. Within the first month after construction, the percolation rate was ≤13 mm/year, but increased to 300 mm/year over the next 4–7 months. Within 2–5 years after installation, average percolation rates of 203–262 mm/year were recorded from the two lysimeters. Based on these percolation rates, the calculated k values of the GCL (assuming a unit hydraulic gradient) were 6.4×10^{-9} to 8.3×10^{-9} m/s (about two orders of magnitude higher than k for a virgin GCL). During reconstruction activities, the seams between the GCL panels were inspected and found to have appropriate overlaps and GCL samples were exhumed from the area inside and outside the two lysimeters after approximately 2 and 5 years of installation to assess k of the GCL in the laboratory using flexible wall permeameters (FWPs) at a hydraulic gradient of 100 and effective stress of 15 kPa. The permeant used was a 10 mmol/L CaCl$_2$ solution. The measured k for samples exhumed after 2 years was 8.7×10^{-8} to 2.4×10^{-7} m/s, whereas k was 1.4×10^{-7} to 9.1×10^{-7} m/s for samples exhumed after 5 years. Similar to Melchior (2002) and Melchior et al. (2010), the k values measured in the laboratory were 1–2 orders of magnitude higher than the k values anticipated from the percolation calculations. Benson et al. (2007) indicated that the in situ downward gradient conditions only occur for short periods of time and the assumption of a unit downward hydraulic gradient for calculating k based on lysimeter readings may give lower k values. Another explanation for the difference between k measured in the laboratory and the in situ k is that the testing conditions in the laboratory may overestimate the in situ k value of GCL by several orders of magnitude.

One of the main differences between the laboratory test conditions versus those in the field is the hydraulic gradient. Most of the post-exhumation k tests on the exhumed specimens have been conducted using hydraulic gradients much higher than those expected under field conditions and sometimes even higher than the values recommended by the applicable American Society of Testing and Materials (ASTM) standards. Although Shackelford et al. (2000) reported that k of GCL was not affected by the hydraulic gradient for values up to 540, this conclusion was reached for virgin GCL specimens permeated in the laboratory using distilled water or 0.6–2.0 mol/L NaCl solution. Thus, these specimens had not experienced any cation exchange and (or) exposure to freeze–

thaw or wet–dry cycles before permeation, as would be expected for shallow covered samples exhumed from the field after several years. This leaves an open question as to what the effect is of hydraulic gradient on k for GCLs exhumed from the field after being exposed to cation exchange and weathering conditions.

Unlike the percolation rates reported in Melchior (2002), Melchior et al. (2010), and Benson et al. (2007), Wagner and Schnatmeyer (2002) reported much lower percolation rates through a cover containing a needle-punched GCL used as a single liner for a blast furnace dust landfill in Luxembourg, Belgium. The assessment of the cover performance involved measuring the leakage through the in situ test cover underlain by a 45 m² lysimeter (3 m × 15 m) over a 2 year period (cover inclination was 5% and the total precipitation on the test plot was 713–1037 mm/year). Two layers of coarse electric furnace slag (by-product of the steel-making process; grading of 4–8 mm), 0.15 and 0.25 m thick, were placed below and above the GCL, respectively, to act as drainage layers. In addition, a 0.75 m layer of silty sand was placed above the top 0.25 m layer of slag to increase the overburden stress above the GCL and protect its integrity. In the first year, the seepage rate through the GCL was 1.4 mm/year, with a maximum daily percolation rate of <0.01 mm/day. In the second year, the seepage rate increased to 6.2 mm/year (maximum daily percolation rate was 0.07 mm/day). Based on these measurements, the calculated k values were in the range of 4×10^{-11} to 2×10^{-10} m/s (assuming unit hydraulic gradient). The significantly improved hydraulic performance of this cover system compared to the previously discussed cases may arise from one or more of the following differences between the conditions examined in the three cases: (*i*) the presence of a drainage layer above and below the GCL that may be expected to have minimized the differential head, ΔH, across the GCL, (*ii*) the greater thickness of cover soil, (*iii*) the nature and length of exposure, and (*iv*) the particular GCL product used.

Benson et al. (2010) evaluated the engineering properties of two needle-punched GCL products exhumed after 4.7–5.8 years in a landfill cover. One GCL had fine granular bentonite and needle-punched fibres that were thermally fused to the woven carrier geotextile and the other GCL had coarse granular bentonite and the needle-punched fibres were not thermally treated. The cover comprised (from top to bottom): 0.3 m of top soil, 0.62–0.92 m of silty sand, a geomembrane, and a GCL. The subgrade soil was silty clay and the porewater was characterized by an ionic strength of 3–5 mmol/L and was dominated by divalent cations (the ratio of the molar concentrations of monovalent cations (M_M) to divalent cations (M_D), or RMD ($M_M/M_D^{0.5}$), = 0.032–0.038 (mol/L)$^{1/2}$). The k values obtained using FWPs under an effective stress of 24 kPa and hydraulic gradient of 125 increased from $1.2–2.6 \times 10^{-11}$ m/s (virgin) to 2.8×10^{-8} m/s for four specimens (both products), whereas k of seven specimens (both products) was almost unchanged ($1.4–4.7 \times 10^{-11}$ m/s) despite a significant reduction in the ESP from 65%–74% (virgin) to 1%–3% for both products and a reduction in the SI of all exhumed samples from 25–36 mL/2 g (virgin) to 8–11 mL/2 g. The reason for the wide range of the measured k values for these products was not reported; however, inspection of the k-tested GCL specimens indicated that there was preferential flow through the needle-punched fibres of the four specimens that experienced a large increase in k.

Similarly, Scalia and Benson (2011) investigated the performance of five different GCL products exhumed from four composite barriers in landfill final covers after 4.7–6.7 years under 0.3–1.1 m of cover soil (thickness varied with the site examined) to evaluate the in-service condition. The SI of GCLs exhumed from two sites dropped to 8–11 mL/2 g, whereas GCLs from the other two sites had an SI of 12–22 mL/2 g. The k values of all GCLs varied over nearly 5 orders of magnitude (1.2×10^{-11} to 2.1×10^{-7} m/s) when tested under 15–24 kPa effectives stress and a hydraulic gradient of 125 using a 10 mmol/L CaCl$_2$ solution as a permeant. There was no clear trend for the relationship between k and the chemical characteristics of the exhumed

Table 1. Initial properties of virgin GCLs.

Property	GCL1	GCL2	GCL3	GCL4
As-delivered form	Fine granular	Fine granular	Coarse granular	Coarse granular
Mineralogy (%)				
Montmorillonite	96	96	84	77
Feldspar	3	2	7	8
Quartz	1	2	4	5
Mica	—	—	4	5
Cristobalite	—	—	1	5
Avg. dry bentonite mass/area, M_b (g/m²)				
Measured[a]	4500 (SD = 400, n = 26)	4600 (SD = 600, n = 26)	4500 (SD = 650, n = 21)	4500 (SD = 500, n = 21)
MARV[b]	3660	3660	3600	3600
Carrier GTX				
Type	W	NWSR	W	NW
Mass (g/m²)[a]	123 (SD = 13, n = 5)	260 (SD = 13, n = 5)	135 (SD = 20, n = 5)	210 (SD = 5, n = 5)
Cover GTX				
Type	NW	NW	NW	NW
Mass (g/m²)[a]	231 (SD = 17, n = 5)	232 (SD = 5, n = 5)	280 (SD = 10, n = 5)	270 (SD = 10, n = 5)
Structure				
Needle-punched	Yes	Yes	Yes	Yes
Thermally treated	Yes	Yes	No	No
Initial (off roll) thickness (mm)[a]	7.7 (SD = 0.6, n = 260)	6.0 (SD = 1, n = 1275)	7.5 (SD = 1, n = 255)	7.5 (SD = 1, n = 255)
Initial (off roll) water content (%)[a]	6 (SD = 1, n = 5)	6 (SD = 2, n = 10)	18 (SD = 6, n = 5)	23 (SD = 2, n = 5)
W_{ref} (%)[c]	116	105	128	143
Hydraulic conductivity (m/s)[d]	3.8×10^{-11}	4.4×10^{-11}	4.3×10^{-11}	5.9×10^{-11}

Note: All tests conducted according to the relevant ASTM standards. SD, standard deviation; n, number of samples; W, woven; NWSR, nonwoven scrim-reinforced; NW, nonwoven.

[a]Values given are average when multiple tests were performed.

[b]Manufacturer's published minimum average roll value (MARV).

[c]Reference water content; represents maximum water content likely attained by the GCL under 15 kPa confining stress when hydrated with a 5 mmol/L $CaCl_2$ solution similar to the pore water in the soil in the field.

[d]At effective stress of 15 kPa, head across the GCL = 1.2 m, and 10 mmol/L $CaCl_2$ solution used as a permeant.

GCLs. For example, one sample had an SI of 18 mL/2 g and k of 1.9×10^{-8} m/s (no preferential flow reported for this specific sample), whereas another sample from the same site had an SI of 8 mL/2 g and k of 4.2×10^{-11} m/s. Similar to the observation reported by Benson et al. (2010), there was preferential flow of the permeant through the needle-punched fibres in some cases during the k test. However, the reason why this preferential flow occurred in some cases and not for others was not indicated.

To understand the flow pattern through a GCL, Scalia and Benson (2010b) hydrated a virgin GCL with dye-spiked distilled water and captured images of the cross section of the GCL during the hydration process every 5 s for 60 min. Within 1 min, the water migrated up through the fibre bundles and reached the cover geotextile before significant hydration of the bentonite. Afterwards, the bentonite hydrated radially from the fibre bundles and vertically from the carrier and cover geotextiles.

Based on the foregoing, it may be hypothesized that the cation exchange initially occurred around the fibre bundles, thereby reducing the swelling capacity of the bentonite around the bundles and preventing bentonite from surrounding and filling space between the fibres in the bundles. Based on the observations described earlier for the possible effect of the hydraulic gradient on the hydraulic conductivity of GCL and the hydration pattern described by Scalia and Benson (2010b), the combination of high hydraulic gradient, cation exchange, and wet–dry or freeze–thaw cycles may be hypothesized to cause changes in the bentonite around the bundles, thereby providing a potential preferential flow conduit. Nevertheless, quantitative explanation for when this may occur cannot be drawn.

The objective of this paper is to examine the chemical and hydraulic performance of GCLs used in a cover application as a single liner and exposed to natural weathering conditions. To achieve these goals, a long-term study was initiated in 2006 by constructing an experimental test cover at the Queen's University Environmental Liner Test Site (QUELTS) in Godfrey (north of

Kingston), Ontario, Canada, at latitude of 44°34′14″N and longitude of 76°39′44″W (Brachman et al. 2007). A 20 m wide × 76 m long cover comprising four different GCL products (used as a single barrier) was constructed on a north-facing side slope (3:1, horizontal to vertical) of silty sand. The GCL layer was covered by 0.7 m of the same silty sand soil used as the foundation soil. The GCL panels were exposed at a number of locations and the physical conditions of the GCL overlaps were examined at both 5 and 7 years after installation. In addition, GCL samples were exhumed from each product to inspect the bentonite structure and measure the chemical and hydraulic characteristics of the four different, but commonly used, GCLs that had been subjected to essentially the same exposure conditions. An additional objective is to investigate the effect of the (i) laboratory test conditions (i.e., applied hydraulic head) and (ii) characteristics of needle-punched bundles on the measured k values of exhumed GCL samples.

Materials

GCLs

The four GCL products examined are denoted as GCL1, GCL2, GCL3, and GCL4 (Table 1). GCL1 (Bentofix Thermal Lock "NSL") was a needle-punched GCL comprising a layer of fine granular Wyoming sodium bentonite between a slit-film woven carrier geotextile (GTX) and a staple fibre nonwoven cover GTX. GCL2 (Bentofix Thermal Lock "SRNWL") was a needle-punched GCL comprising a layer of fine granular Wyoming sodium bentonite encapsulated between a scrim-reinforced nonwoven carrier GTX (a woven slit-film GTX and a nonwoven GTX needle-punched together) and a staple fibre nonwoven cover GTX. Needle-punched fibres in GCL1 and GCL2 were thermally treated to enhance the bond to the carrier GTX. GCL3 (Bentomat "ST") consisted of a layer of coarse granular Wyoming sodium bentonite encapsulated between a slit-film woven carrier GTX and a staple fibre nonwoven cover GTX. GCL4 (Bentomat "DN") was similar to GCL3 except that the carrier

GTX was nonwoven. The needle-punched fibres in GCL3 and GCL4 were not thermally treated. The colour of the carrier GTXs in GCL1 and GCL2 was white, whereas carrier GTXs were black for GCL3 and GCL4.

The mineralogy of the bentonite in virgin GCLs was analyzed using 0.2 g of air-dried bentonite samples that were scanned with a Panalytical X'Pert Pro MPD diffractometer fitted with an X'Celerator high-speed strip detector and K-beta filtered Co radiation (wavelength, λ = 1.79 Å). The bentonite was ground to a powder finer than 75 μm; a portion of the powder was mounted with methanol as a thin oriented smear on a glass disk. Samples were scanned from 4° to 70° 2θ using a count time of 10 s/° at 0.02° increments and a sample rotation of 2 s/revolution. PANAlytical HighScore Pro software was used for phase identification; the software compares the peak positions and peak intensities to data in the large International Centre of Diffraction Data (ICDD) PDF2+ database of known phases. In addition, a semi-quantitative determination of the percentage of the major minerals in the bentonite samples was performed using integrated peak areas and reference intensity ratio factors. The dominant mineral in GCL1 and GCL2 was montmorillonite (96%), whereas the nonclay minerals were feldspar (2%–3%) and quartz (1%–2%). The smectite content of the bentonite used in GCL3 and GCL4 varied between 77% and 84% with 7%–8% feldspar, 4%–5% mica, 4%–5% quartz, and 1%–5% cristobalite.

Two different techniques were followed to investigate the characteristics of the needle-punched bundles (i.e., the size of the bundles and the number of bundles per unit area) of the four tested GCLs. The first technique involved placing GCL samples (0.3 m × 0.3 m) from each product on a light table in a dark room and taking high-resolution photographs (resolution = 72 dpi) from above the GCL. The light penetrates through the bundles (which show up white), but not through the bentonite layer (which show up black); thus, the characteristics of the bundles could be quantified by image analysis. The other technique was to measure the size and number of bundles manually for 0.07 m diameter circular samples from each GCL product that were permeated in a FWP with water mixed with blue dye (Brilliant Blue G-250) until the blue-coloured water appeared in the effluent. After test termination, the GCL specimens were cut to expose a representative cross section and the size of at least 20 bundles was measured using a stereoscopic microscope. The number of bundles within the sample was counted manually under the microscope (the blue colour was more concentrated at the bundle locations) and the approximate number of bundles per unit area was then calculated.

Using the light table technique, the average diameter of bundles in GCL1 (Fig. 1a) was 0.7 ± 0.2 mm and there were 114 000 bundles/m², representing 4% of the total surface area of GCL1 (Table 2). The bundles in GCL2 were larger on average than those for GCL1 (Fig. 1b and Table 2), with an average diameter of 1.1 ± 0.5 mm and 94 000 bundles/m², representing 9% of the total surface area of the GCL. Because the carrier GTXs in GCL3 and GCL4 were black, the light would not penetrate through them and the light table technique was not possible for these two specific GCL products.

The average size of bundles for GCL1 and GCL2 based on the manual measurements was 0.5 ± 0.1 mm and 1.0 ± 0.3 mm, respectively, and the number of bundles per unit area counted manually for GCL1 and GCL2 was 100 000 and 80 000 bundles/m², respectively. The difference in the size and number of needle-punched bundles obtained from the two techniques can be attributed to the limitations and errors associated with each technique. However, statistically, the size of bundles measured manually and by the light table technique for each GCL does not differ. The number of bundles per unit area is more accurate based on the light table technique given that the light table technique gave opportunity to estimate the number of bundles based on measurements for a large number of bundles (typically >8000 bundles for a 0.3 m ×

Fig. 1. Light penetrating through needle-punched fibres of (*a*) GCL1 and (*b*) GCL2 when 0.3 × 0.3 m samples were placed on a light table in a dark room (needle-punched fibres appear as white dots).
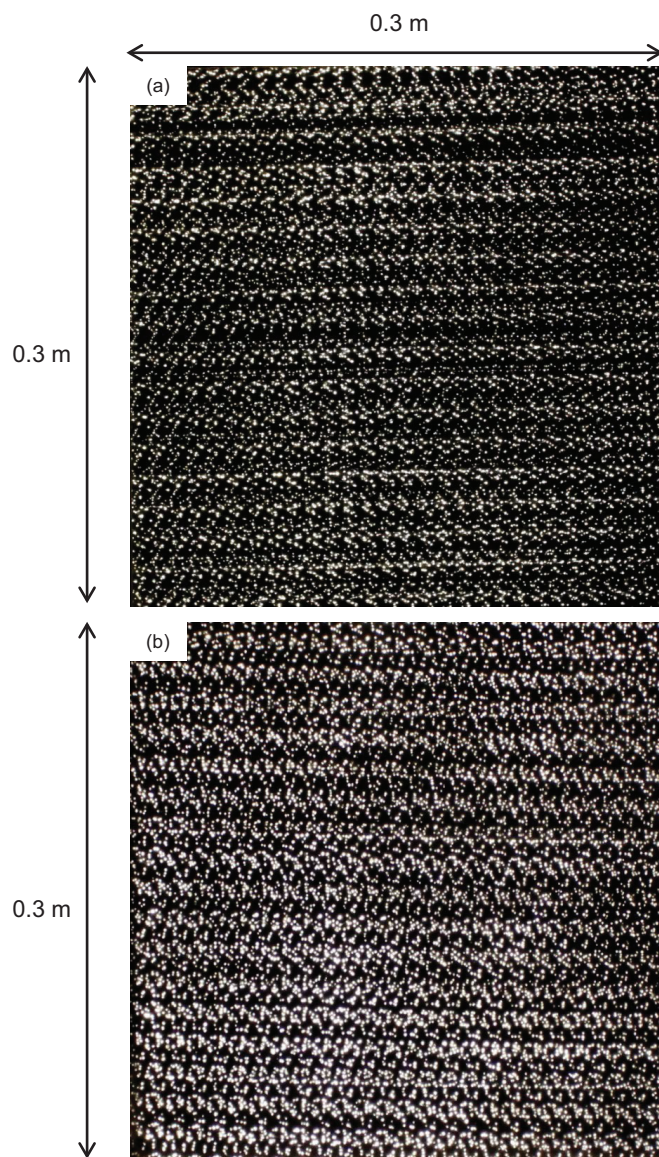
0.3 m sample), whereas the manual measurement was based on only about 20 measurements.

The average sizes of bundles of GCL3 and GCL4 were 1.2 ± 0.2 mm and 1.6 ± 0.5 mm, respectively; and there were 80 000 and 67 000 bundles/m², representing 9% and 14% of the total area of GCL3 and GCL4, respectively. The peel strength increased with increasing bundle diameter (compare GCL1 and GCL2; Table 2) and, for the same bundle size, the GCL with thermally treated bundles exhibited higher peel strength (compare GCL2 and GCL3; Table 2). It is noted that GCL2 and GCL4 with a nonwoven component of the carrier had larger standard deviations in bundle size than GCL1 and GCL3 with a woven carrier. This may be due to some nonwoven fibres being brought back from the carrier when the needles were withdrawn in a more variable manner.

Cover and foundation soil

During the extraction of GCL samples in 2011 (5 years after construction), soil samples were exhumed from above and below the GCL at different depths to obtain the grain-size distribution, water content, density, and chemical composition of the pore-

Table 2. Characteristics of needle-punched fibres for the four tested GCLs.

GCL	Bundle size (mm)[a]	No. of bundles/area (bundles/m²)	No. of fibres/bundle	Area covered by bundles (%)	Avg. bonding peel strength (N/m)	Avg. peak peel strength (N)
GCL1[b]	0.7±0.2	114 000	9	4	662 (SD = 88, n = 5)	94 (SD = 17, n = 5)
GCL2[b]	1.1±0.5	94 000	19	9	2368 (SD = 122, n = 5)	261 (SD = 17, n = 5)
GCL3[c]	1.2±0.2	80 000	27	9	1510 (SD = 256, n = 5)	204 (SD = 35, n = 5)
GCL4[c]	1.6±0.5	67 000	49	14	1780 (SD = 280, n = 5)	219 (SD = 30, n = 5)

[a]Mean ± standard deviation.
[b]Based on the light table technique.
[c]Based on manual measurements using microscope.

Fig. 2. Panel layout, locations where GCL sampling was conducted, and locations where the GCL overlaps were inspected (not to scale).
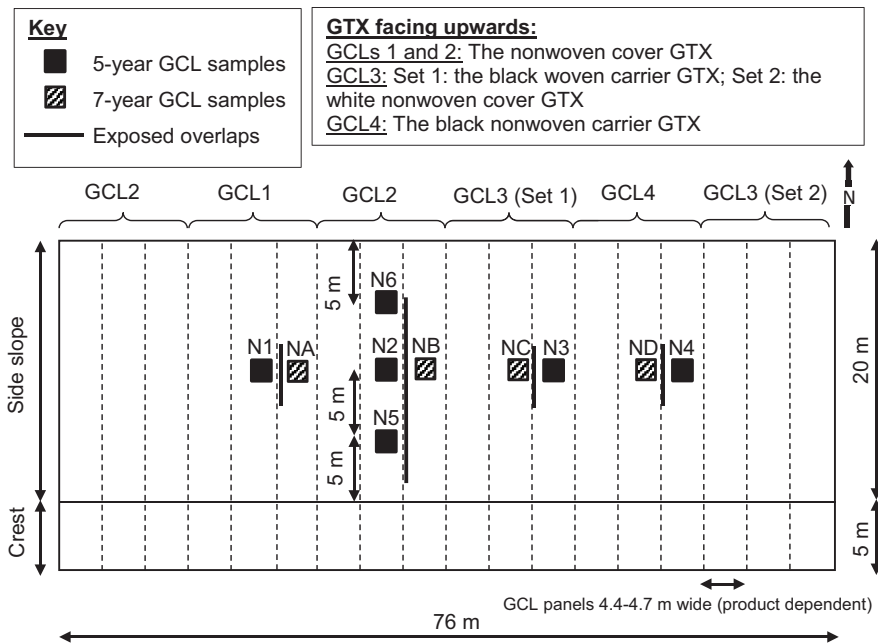
water. Soil samples from above the GCL were collected using a thin-walled cylinder of known volume and the foundation soil was collected using Shelby tubes. The soil above and below the GCL was classified as silty sand according to the *Canadian foundation engineering manual* (CFEM, Canadian Geotechnical Society 2006). The water content above the GCL at the time of exhumation varied between 19% and 24% with an increase in water content with depth (i.e., moisture accumulated above the GCL). The water content was relatively consistent throughout the foundation layer below the GCL at about 18% and, hence, was lower than the average water content above the GCL (22%). The bulk density (mean: 2.1 Mg/m³; range: 2.0–2.2 Mg/m³) and the dry density (mean: 1.75 Mg/m³; range: 1.6–1.85 Mg/m³) of the cover and foundation soil were essentially constant with depth.

The shake flask extraction technique (Price 2009) was followed to measure the readily extractable elements from the exhumed soil samples after 5 years. The average porewater Ca^{2+} concentration for soil samples collected from three different locations was 193 ± 26 mg/L above and 272 ± 23 mg/L below the GCL (with the difference possibly being related in part to movement of ions in the soil above the GCL over the 5 year period due to infiltration being deflected downslope by the GCL rather than deeper into the silty sand and in part to the higher water content in the soil above the GCL than below, which can give a lower concentration for a given dissolved mass of ions in the pore fluid of the soil). The concentrations of Mg^{2+}, Na^+, and K^+ were 27 ± 6, 20 ± 17, and 6 ± 2 mg/L, respectively, above and 43 ± 2, 43 ± 15, and 7 ± 2 mg/L, respectively, below the GCL. No other cations were detected in the extracted water. The ionic strength of the porewater was 15 ± 5 mmol/L, the ratio of the mono-

valent soluble cations (in cmol/kg) to the divalent soluble cations (in cmol/kg) (MDR) was 0.27 ± 0.08, and the total soluble cations per unit mass (TCM) was 1.7 ± 0.4 cmol/kg.

Test cover description

GCLs rolls 4.4–4.7 m wide (product dependent) were placed with three adjacent panels of each product (Fig. 2). All panels were overlapped by 300 mm and 0.4 kg/m supplemental bentonite was placed between the panels at each overlap to improve the seal. GCL3 and GCL4 have a melted groove in the nonwoven cover GTX of the GCL in the longitudinal direction that allows bentonite, upon hydration, to extrude into the overlap zone providing self-seaming in the longitudinal overlaps. Although no supplemental bentonite was required by the manufacturer for GCL3 and GCL4, supplemental bentonite was placed between overlapped panels at a rate of 0.4 kg/m to be comparable to the overlaps for GCL1 and GCL2. To monitor the horizontal separation and downslope movement of each GCL panel relative to the adjacent panels with time (e.g., due to shrinkage, differential settlement of foundation soil), spray paint marks were placed on the overlaps every 2 m from the top of the slope to provide a reference for assessing movement and separation between the panels at overlaps.

Local climatic conditions

Godfrey, Ontario, has a humid continental climate (i.e., Dfb according to the Köppen-Geiger climate classification; McKnight and Hess 2000). Based on the climate characteristics recorded at the closest weather station (44°22′00″N, 76°37′00″W; "Cataraqui TS"

Fig. 3. Daily maximum and minimum temperature profiles in soil above and below GCL on clear, sunny days closest to the start of selected months during period of year where heat is being (*a*) stored and (*b*) released from in the cover soil.
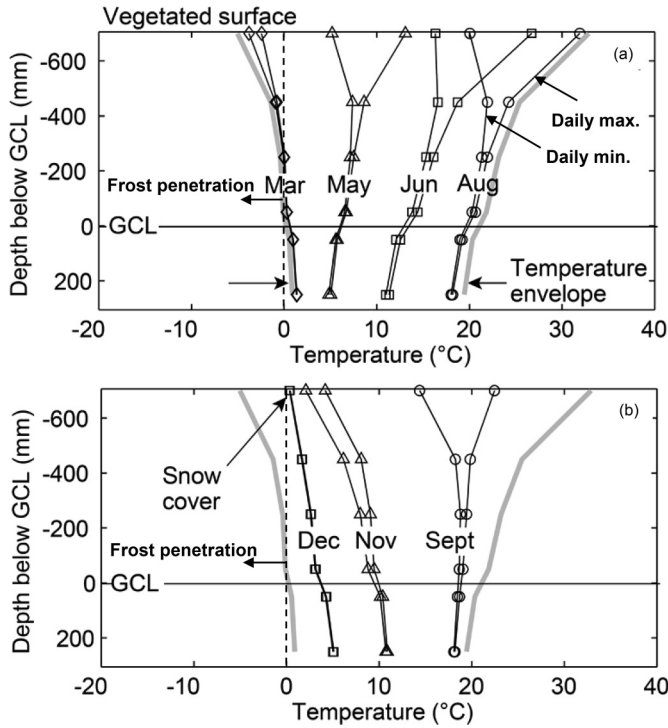
Fig. 4. Annual variation of temperature of GCL placed 700 mm under the cover soil at QUELTS. Minimum GCL temperature between Sept 2006 and Dec 2009 was 0.24 °C. [Colour online.]

Fig. 5. (*a*) Supplemental bentonite at GCL4 overlaps, (*b*) soil intrusion between GCL2 overlapped panels, and (*c*) root penetration through GCL3 overlaps and engineered groove. [Colour online.]
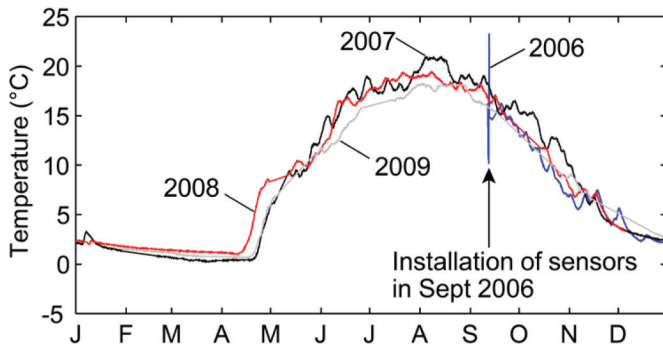
station located about 23 km from the test cover) during the reference period 1971–2000 (Environment Canada 2013), the annual average temperature was 6.6 ± 2.0 °C. The coldest month was January (−8.7 ± 3.3 °C) and the warmest month was July (20.9 ± 1.1 °C). During the period 2006–2011, the annual average temperature was 8.1 °C (varying between −24 °C in January and +30 °C in August).

The average annual precipitation during the reference period 1971–2000 (994 mm) was almost uniformly distributed throughout the year with an average monthly precipitation of 83 ± 10 mm. The month with the most precipitation was September (98.8 mm) and that with the least precipitation was July (65.2 mm). Snow or mixed precipitation of 181 mm/year represented 18% of the average annual precipitation. The annual precipitation during the period 2006–2011 varied between 777 mm (2009) and 1258 mm (2011). The temperature profiles measured for the cover soil at the site for the period from September 2006 to December 2009 indicated that the frost penetration was 0.60–0.65 m (Fig. 3) and the minimum temperature of the soil at the GCL–soil interface was +0.24 °C (Fig. 4); the GCL itself never froze.

Experimental program and test methods

Five years after construction, GCL samples (0.3 m × 0.3 m each) were exhumed from each GCL product (as per ASTM (2008*a*) standard D6072-08) from the middle of the side slope (samples N1–N4 taken 10 m from the top of the slope; Fig. 2). Additional GCL2 samples were exhumed from a location close to the top of the slope (sample N5 taken 5 m down from the crest) and close to the bottom of the slope (sample N6 taken 5 m up from the toe). Similarly, after 7 years of construction, GCL samples from each GCL product (NA to ND; Fig. 2) were extracted from the middle of the slope. During the extraction of the GCL samples 5 and 7 years after

Table 3. Properties of the 5 and 7 year GCL1 specimens before k tests along with the measured k values.

Exposure at field (years)	Specimen condition	Dry bentonite mass/area, M_b (g/m²)	W_c (%)	W_c/W_{ref}[a]	Thickness (mm)	k (m/s)[b] $\Delta H = 0.07$ m	$\Delta H = 0.14$ m	$\Delta H = 0.21$ m	$\Delta H = 0.49$ m	$\Delta H = 0.63$ m	$\Delta H = 1.20$ m
5	Regular	5540	77	0.66	7.9±0.4	—	—	—	—	4.0×10^{-11}	—
		5280	69	0.59	7.5±0.4	6.0×10^{-11}	—	1.3×10^{-10}	—	—	—
		5230	77	0.66	7.7±0.4	1.2×10^{-10}	1.4×10^{-10}	1.4×10^{-10}	1.5×10^{-10}	—	2.2×10^{-10}
	Roots	5650	63	0.54	7.5±0.4	1.4×10^{-10}	1.4×10^{-10}	2.3×10^{-10}	1.7×10^{-10}	—	2.1×10^{-10}
	Thin	4610	61	0.53	5.0±0.7	1.2×10^{-10}	1.4×10^{-10}	1.5×10^{-10}	1.5×10^{-10}	—	1.5×10^{-10}
7	Regular	5400	80	0.69	8.2±0.5	1.6×10^{-10}	1.4×10^{-10}	—	2.7×10^{-7}	—	2.8×10^{-10}
		4950	72	0.62	7.2±0.5	4.1×10^{-10}	1.7×10^{-10}	1.9×10^{-10}	1.9×10^{-10}	—	2.5×10^{-10}
	Bentonite extrusion	3900	84	0.72	5.0±2.0	1.6×10^{-7}	1.3×10^{-7}	1.8×10^{-7}	—	—	—

[a]W_{ref} of GCL1 = 116% at 15 kPa.
[b]Hydraulic conductivity measured in FWP using 10 mmol/L $CaCl_2$ solution as permeant.

Table 4. Properties of the 5 and 7 year GCL2 specimens before k tests along with the measured k values.

Exposure at field (years)	Specimen condition	Dry bentonite mass/area, M_b (g/m²)	W_c (%)	W_c/W_{ref}[a]	Thickness (mm)	k (m/s)[b] $\Delta H = 0.07$ m	$\Delta H = 0.14$ m	$\Delta H = 0.21$ m	$\Delta H = 0.49$ m	$\Delta H = 0.63$ m	$\Delta H = 1.20$ m
5	Regular	5340	58	0.55	7.4±0.4	6.5×10^{-11}	8.0×10^{-11}	4.2×10^{-9}	4.4×10^{-9}	—	2.0×10^{-9}
		5990	66	0.63	9.1±0.9	4.8×10^{-10}	1.6×10^{-9}	1.1×10^{-9}	1.2×10^{-9}	—	2.0×10^{-9}
		5700	66	0.63	8±1	7.1×10^{-10}	2.4×10^{-9}	1.6×10^{-9}	2.7×10^{-9}	—	6.1×10^{-9}
	Thin	4410	53	0.50	7.0±0.3	—	—	—	—	4.6×10^{-8}	—
		4860	54	0.51	7.2±0.5	5.8×10^{-11}	—	2.5×10^{-8}	2.8×10^{-8}	—	4.9×10^{-8}
		4560	59	0.56	5.8±0.5	2.7×10^{-10}	8.7×10^{-10}	3.9×10^{-8}	1.2×10^{-7}	—	2.0×10^{-7}
		4750	71	0.68	7.0±0.5	1.9×10^{-10}	1.9×10^{-10}	2.6×10^{-8}	2.7×10^{-8}	—	2.7×10^{-8}
		4480	75	0.71	6.7±0.3	2.2×10^{-10}	7.1×10^{-10}	3.0×10^{-8}	6.3×10^{-8}	—	6.8×10^{-8}
	Roots	5710	59	0.56	6.9±0.4	7.2×10^{-11}	8.5×10^{-11}	4.2×10^{-9}	8.9×10^{-9}	—	1.7×10^{-8}
7	Thin	4300	78	0.74	7.3±0.2	3.2×10^{-9}	2.8×10^{-8}	—	3.4×10^{-8}	—	5.0×10^{-8}
	Regular	4950	67	0.63	6.9±0.5	5.4×10^{-10}	2.0×10^{-9}	4.8×10^{-9}	4.8×10^{-9}	—	5.2×10^{-9}

[a]W_{ref} of GCL2 = 105% at 15 kPa.
[b]Hydraulic conductivity measured in FWP using 10 mmol/L $CaCl_2$ solution as permeant.

Table 5. Properties of the 5 and 7 year GCL3 specimens before k tests along with the measured k values.

Exposure at field (years)	Specimen condition	Dry bentonite mass/area, M_b (g/m²)	W_c (%)	W_c/W_{ref}[a]	Thickness (mm)	k (m/s)[b] $\Delta H = 0.07$ m	$\Delta H = 0.14$ m	$\Delta H = 0.21$ m	$\Delta H = 0.49$ m	$\Delta H = 1.20$ m
5	Regular	5190	67	0.52	7.9±0.4	7.6×10^{-11}	—	4.3×10^{-8}	4.7×10^{-8}	6.1×10^{-8}
		5590	77	0.60	8.4±0.6	8.0×10^{-11}	6.0×10^{-8}	2.6×10^{-8}	2.6×10^{-8}	2.7×10^{-8}
	Cracked	4870	72	0.56	7±1	6.3×10^{-10}	4.1×10^{-8}	6.6×10^{-8}	4.9×10^{-8}	5.4×10^{-8}
	Roots	5800	77	0.60	9±1	2.7×10^{-10}	4.1×10^{-8}	3.5×10^{-8}	3.9×10^{-8}	4.1×10^{-8}
7	Regular	5300	55	0.43	7.8±0.5	7.0×10^{-10}	2.0×10^{-8}	—	7×10^{-8}	7.3×10^{-8}
		5400	59	0.46	8±1	3.8×10^{-10}	3.0×10^{-9}	1.3×10^{-9}	4.0×10^{-9}	4.1×10^{-9}

[a]W_{ref} of GCL3 = 128% at 15 kPa.
[b]Hydraulic conductivity measured in FWP using 10 mmol/L $CaCl_2$ solution as permeant.

construction, the overlaps at 10 and 12 m from the top of the slope for all GCLs were exposed and the lateral and downward movements were measured. In addition, the movements at 4, 6, 14, and 16 m from the top of the slope were measured for GCL2.

Before testing, each exhumed GCL specimen was X-rayed using a 1 kV X-ray imager to capture high-resolution radiographs (resolution up to 7 LP/mm) of the bentonite structure. After the visual and X-ray inspection of the bentonite, the SI and exchangeable cations of the exhumed bentonite were measured. The SI tests were conducted according to ASTM (2006) standard D5890-06, except that air-dried bentonite was used instead of oven-dried bentonite to avoid any change in bentonite mineralogy (Gu et al. 2001; ASTM (2010) standard D7503-10; Hosney and Rowe 2013). ASTM (2010) standard 7503-10 was followed to obtain the soluble cations,

bound cations, and cation exchange capacity of bentonite from the exhumed GCL samples. An inductively coupled plasma-mass spectrometer was used for chemical analysis of the extracts from the soluble cations and bound cations stages. The concentration of the ammonia was measured in the extract from the cation exchange capacity stage using an autoanalyzer to quantify the nitrogen in the extract and calculate the cation exchange capacity.

Based on the visual and X-ray inspection of the bentonite structure, 0.07 m diameter circular GCL specimens were cut from the exhumed samples from locations (*i*) with no cracks or any visible defects in the bentonite structure or any penetrated roots (denoted as regular specimens); (*ii*) where the bentonite was thin or cracked; and (*iii*) where roots penetrated through the GCL. The k

Table 6. Properties of the 5 and 7 year GCL4 specimens before k tests along with the measured k values.

Exposure at field (years)	Specimen condition	Dry bentonite mass/area, M_b (g/m²)	W_c (%)	$W_c/W_{ref}{}^a$	Thickness (mm)	k (m/s)^b $\Delta H = 0.07$ m	$\Delta H = 0.14$ m	$\Delta H = 0.21$ m	$\Delta H = 0.49$ m	$\Delta H = 1.20$ m
5	Regular	5340	63	0.44	7.7±0.3	8.6×10^{-11}	—	1.5×10^{-7}	1.7×10^{-7}	2.1×10^{-7}
		5140	74	0.52	7.7±0.3	9.9×10^{-11}	4.6×10^{-8}	1.2×10^{-7}	1.5×10^{-7}	1.5×10^{-7}
	Cracked	4810	71	0.49	8.9±0.6	3.9×10^{-9}	1.2×10^{-7}	1.0×10^{-7}	1.1×10^{-7}	1.2×10^{-7}
	Roots	5490	76	0.53	9±1	1.3×10^{-9}	1.1×10^{-7}	1.8×10^{-7}	1.6×10^{-7}	2.0×10^{-7}
7	Regular	4900	75	0.52	8.5±0.5	1.1×10^{-10}	3.7×10^{-8}	—	2.7×10^{-7}	4.9×10^{-7}
		5900	86	0.60	10±1	1.0×10^{-10}	4.0×10^{-8}	4.0×10^{-7}	4.0×10^{-7}	4.0×10^{-7}

$^a W_{ref}$ of GCL4 = 143% at 15 kPa.
^{b}Hydraulic conductivity measured in FWP using 10 mmol/L CaCl$_2$ solution as permeant.

Fig. 6. (*a*) Typical bentonite structure at exhumation for GCLs 1 and 2, (*b*) cross section of GCL4 showing the bentonite granules observed in GCLs 3 and 4, and (*c*) cracks observed in GCL3 (similar cracks were observed in GCL4). [Colour online.]
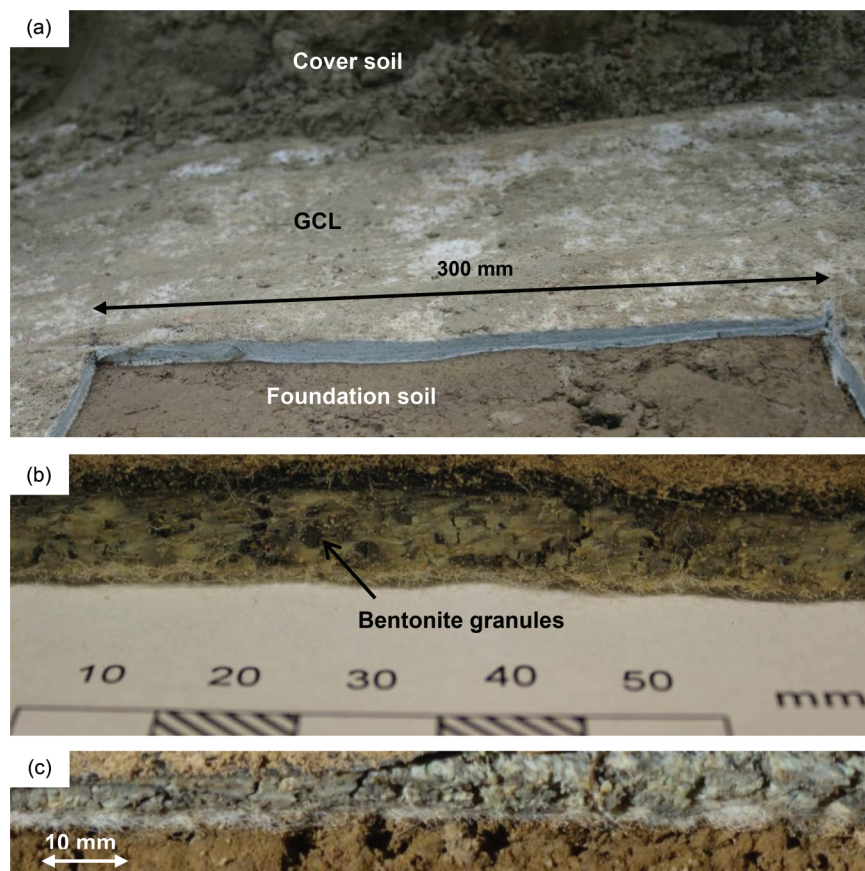
value of the extracted specimens was then measured using FWPs under falling-head – rising-tail conditions following ASTM (2004) standard D5084-03. For all k tests using a nonstandard permeating liquid (i.e., any liquid other than tap water), bladder accumulators were used as interface chambers. The average confining pressure acting on all tested GCLs was 15 kPa (cell pressure of 179.2 kPa, influent pressure value ranged from 164.7 to 170.3 kPa, and effluent pressure value varied between 164.1 and 158.6 kPa). The values of the influent and effluent were selected to achieve the target average confining pressure. Two test series were conducted as described below.

In the first test series, a 10 mmol/L CaCl$_2$ synthetic solution was used as a permeant (400 mg/L Ca²⁺ and 700 mg/L Cl⁻; i.e., almost double the Ca²⁺ concentration in the porewater of the cover soil at the test cover, but similar to permeating liquid used by Benson et al. 2010). The initial differential synthetic water head across the

GCL specimens was 0.07 m (simulating a possible water head in the field when there is a drainage layer above the GCL). To investigate the effect of the hydraulic gradient on the measured k values, once k reached steady-state under a 0.07 m head, the differential head was increased incrementally to 0.14, 0.21, 0.49, and 1.2 m (gradients of about 9, 18, 27, 64, and 158 for 0.07, 0.14, 0.21, 0.49 and 1.2 m, respectively) and k was allowed to reach steady-state at each stage.

In the second test series, the differential head across the GCL specimen was held constant at 0.07 m and three different permeants were used. Initially, each specimen was permeated with tap water (1 mmol/L Ca²⁺). When k stabilized, the permeant was switched to a 5 mmol/L CaCl$_2$ solution (200 mg/L Ca²⁺; the average Ca²⁺ concentration measured in the porewater of cover soil) followed by a 10 mmol/L CaCl$_2$ solution. At the end of each k test and before termination, the permeating liquid was spiked with blue

dye to allow observation for the flow pattern through tested GCL specimens.

Results and discussion

Performance of GCL overlaps

The horizontal separation and downslope movement of GCL panels were measured at different locations. For GCL1, GCL3, and GCL4, there was no measurable horizontal separation between panels (<1 mm) at 10 and 12 m from the top of the slope 5 and 7 years after construction. For GCL2, the horizontal separation after 5 and 7 years varied in a narrow range from <1 mm to 8 mm, and this was most likely due to movement when the cover soil was placed. Thus, under a cover thickness of 0.7 m, there was no significant shrinkage of the four GCLs (<8 mm at panel overlaps) after 7 years. The downward movement of all GCL panels varied between <5 mm and 35 mm. This downward movement likely occurred during the placement of the cover soil above the GCL, as there was no significant apparent differential settlement. Thus, the GCL overlaps were still physically intact after up to 7 years under the exposed field conditions with negligible movements.

Inspection of the overlaps indicated that, for all GCLs, the supplemental bentonite was typically well hydrated with no visible macro features (e.g., Fig. 5a). However, there was 70 mm of soil intrusion below the upper panel at an overlap (Fig. 5b) located 4 m from the top of the slope; this was not typical and was observed at only one location. This soil intrusion most likely took place during the placement of the cover soil during construction. Fine roots frequently penetrated laterally through the supplemental bentonite at overlaps (Fig. 5c). There was no bentonite extruded from the melted groove for GCL3 and CGL4 (Fig. 5c), although the exhumed water content of the bentonite in both GCLs after 5 and 7 years was typically ≈70%. In this case, that would not have affected performance because the overlap was 300 mm and 0.4 kg/m of supplemental powdered bentonite had been placed; however, it does raise questions about performance if only a 150 mm overlap and no supplemental bentonite had been used. Based on the field observations, there was no evidence that the hydraulic performance of the 300 mm overlaps with 0.4 kg/m of supplemental had been compromised.

Water content and mass per unit area of exhumed GCLs

Tables 3–6 give the dry bentonite mass per unit area (M_b), water content (W_c), and thickness of the exhumed GCLs. Following Rayhani et al. (2011), the W_c values were normalized by their hydration potential (denoted herein as reference water content, W_{ref}), which represents the maximum water content to which a GCL is expected to hydrate under a specific stress and specific liquid. To obtain W_{ref}, 0.3 m × 0.3 m GCL samples were immersed in a 5 mmol/L CaCl$_2$ solution (200 mg/L Ca^{2+}; similar to Ca^{2+} concentration of the cover soil porewater at the site) under 15 kPa stress and the water content at equilibrium (W_{ref}; Table 1) was used to calculate the ratio W_c/W_{ref} (Tables 3–6), which approximates the degree of potential hydration at these conditions (i.e., for this permeant and stress level).

For GCL1 samples exhumed after 5 and 7 years (Table 3), the average M_b was 5100 ± 600 g/m^2, which was greater than both the manufacturer's published minimum average roll value (MARV) and the average measured value for virgin GCL1 (Table 1). The exhumed W_c varied between 61% and 84% (average = 73% ± 8% (arithmetic mean ± standard deviation)), which corresponded to W_c/W_{ref} of 62% ± 7%. There was no significant statistical difference between M_b and W_c measured for the 5 and 7 year samples.

The average M_b of the exhumed GCL2 samples (Table 4) was 5000 ± 600 g/m^2, which was well above both the MARV and average measured initial value. The average exhumed W_c was 63% ± 8% (W_c/W_{ref} of 60% ± 8%). Therefore, samples exhumed from both

Fig. 7. Roots running (a) above and (b) below GCL layer; and (c) roots that had penetrated through the cover geotextile and bentonite then ran along the lower bentonite and carrier geotextile interface (desiccation is due to oven drying). [Colour online.]
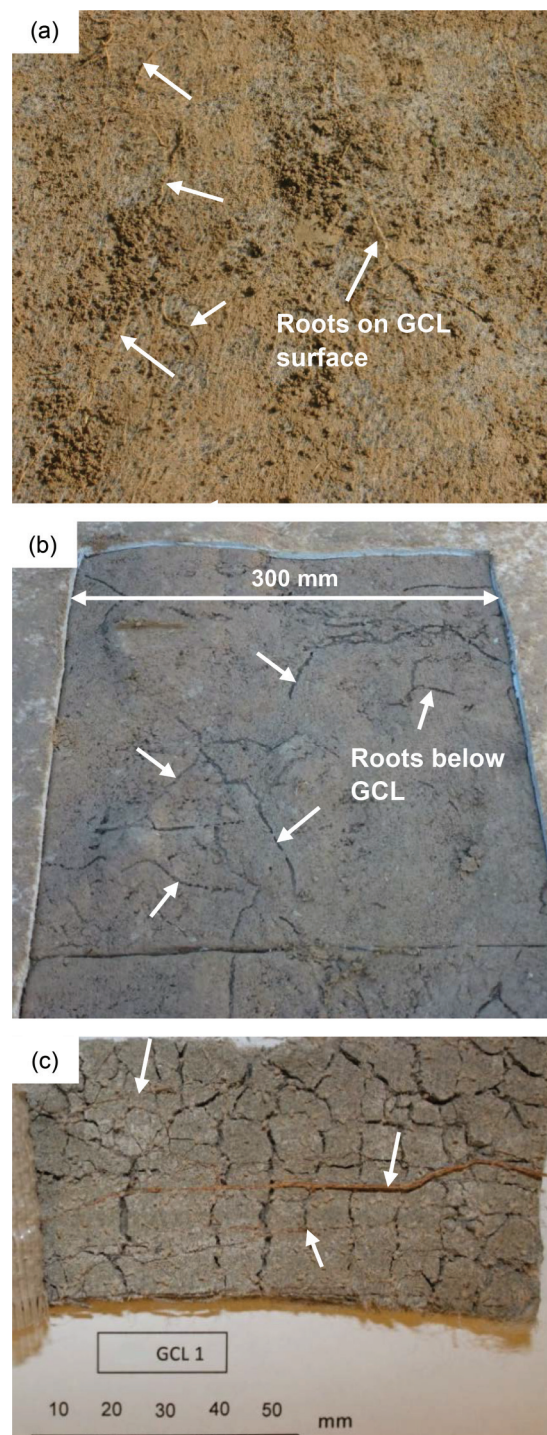
GCL1 and GCL2 have almost the same average M_b (5000–5100 g/m^2) and degree of saturation (W_c/W_{ref} of about 60%).

The average M_b of both GCL3 (5400 ± 300 g/m^2; Table 5) and GCL4 (5300 ± 400 g/m^2; Table 6) was greater than average measured values for GCL1 and GCL2. The average exhumed W_c values for both products were 67% (range: 55%–77%) with W_c/W_{ref} of 52% ± 7% for GCL3 and 74% (range: 63%–86%) with W_c/W_{ref} of 51% ± 5% for

Fig. 8. X-ray images for GCL1 exhumed after (*a*) 5 years and (*b*) 7 years.
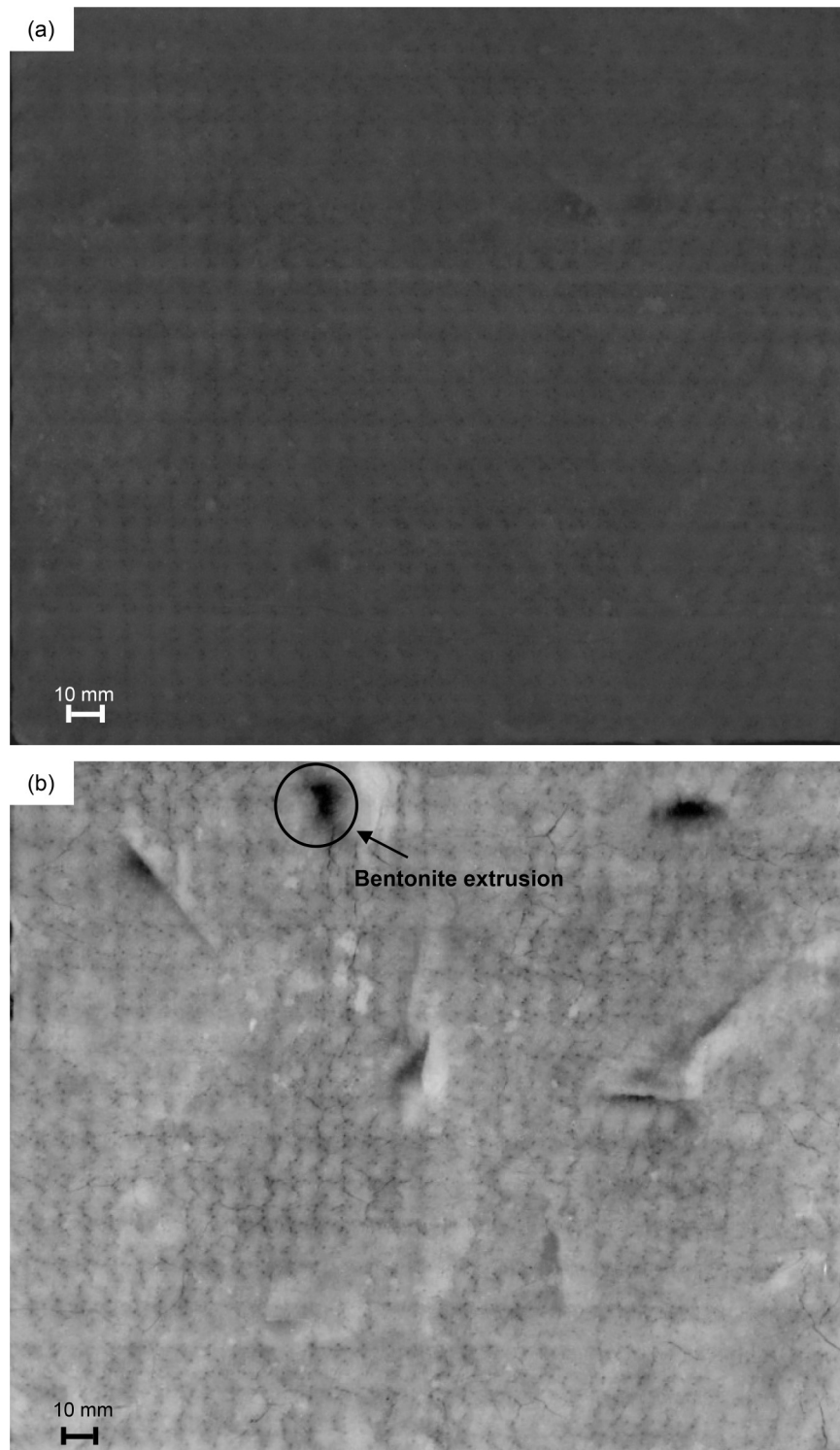
GCL4. Thus, the exhumed degree of saturation (W_c/W_{ref}) of GCL3 and GCL4 was less than that measured for GCL1 and GCL2.

Visual and X-ray inspection of exhumed GCLs

On visual inspection, the exhumed GCL1 and GCL2 (with fine granular bentonite) samples appeared to be consistently sufficiently hydrated to have a gel-like structure and there were no visible defects in the GCL components (bentonite and geotextiles)

or evidence of cracks or flocculation in the bentonite structure (Fig. 6*a*). In contrast, at lower W_c/W_{ref} values than those measured for GCL1 and GCL2, the bentonite in GCL3 and GCL4 (with coarse granular bentonite) did not appear well hydrated and there were some partially hydrated bentonite granules with macrovoids (i.e., gaps) between the granules that were visually evident in GCL4 (Fig. 6*b*). Occasional macrofeatures like tiny cracks in the bentonite were also evident in GCL3 and GCL4

Fig. 9. Sample N5 (GCL2): (*a*) top, (*b*) foundation below sample, and (*c*) X-ray image. [Colour online.]
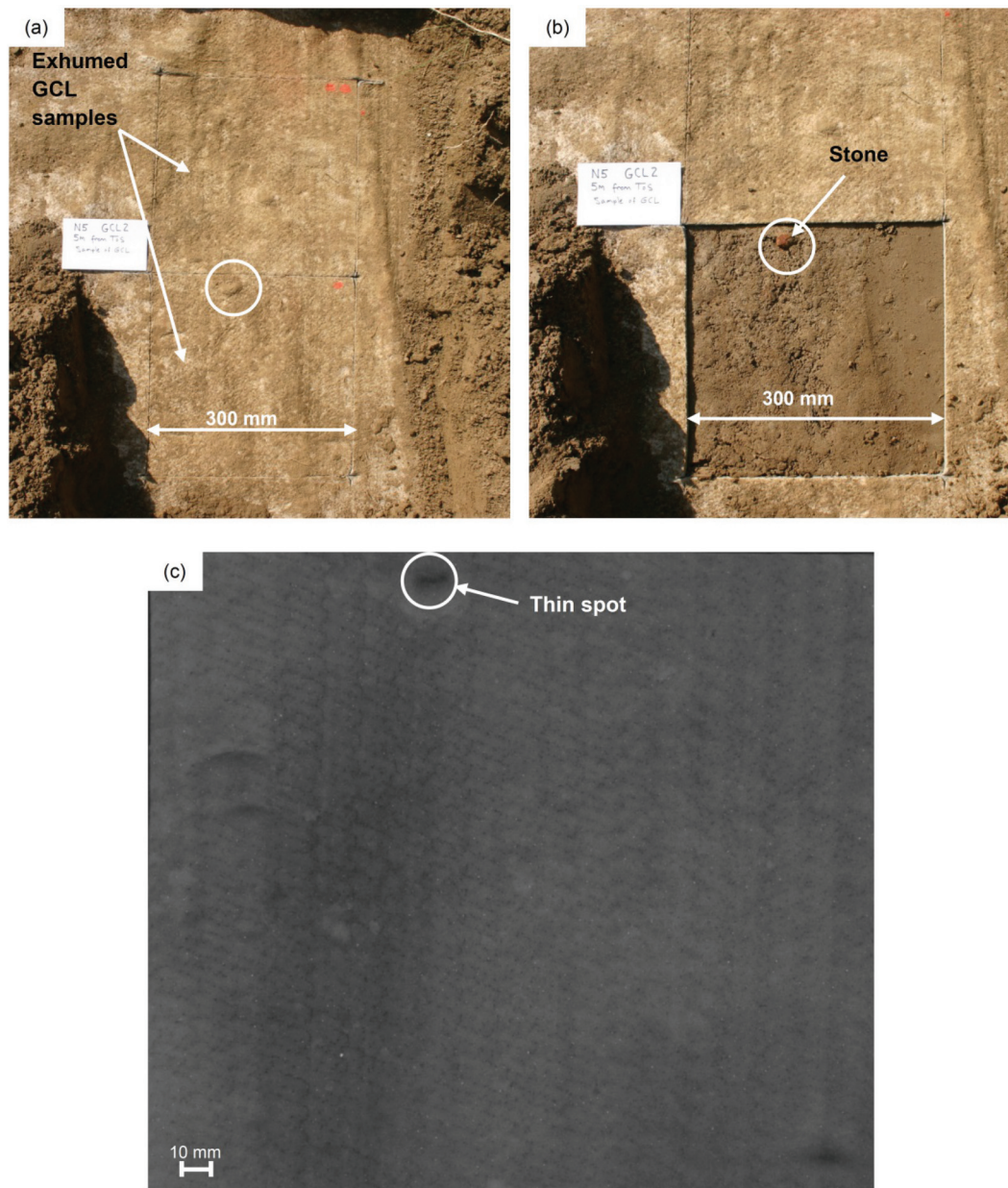
(Fig. 6c). Thus, whereas the bentonite particles had taken up moisture, they had not taken up sufficient moisture to form a consistent gel structure.

Many roots were observed running along the top–cover (Fig. 7a) and the bottom–carrier (Fig. 7b) geotextiles of GCL for all exhumed GCL samples. To inspect the penetration of roots through GCLs, specimens from the exhumed GCL samples were oven-dried and the carrier and cover geotextiles carefully removed. Several tiny roots were running laterally along the interface between the geotextiles and the bentonite layer (Fig. 7c).

Consistent with the visual inspection, there were no cracks in the bentonite of GCL1 and GCL2 evident in the X-ray images (e.g., Fig. 8a). However, there were occasional locations where the bentonite had thinned relative to the rest of the sample or the bentonite had been extruded (Fig. 8b). The thin or bentonite extrusion spots were associated with irregularities in the foundation soil. For example, during the extraction of sample N5 (GCL2), a local

bump was observed in the GCL surface (Fig. 9a). When the GCL sample was extracted, a stone (20 mm × 15 mm, thickness = 5–10 mm) in the foundation layer was responsible for this bump (Fig. 9b). The X-ray image for this sample showed that, directly above the stone, the thickness of the GCL had been reduced relative to the rest of the sample (Fig. 9c). To quantify the thinning in this GCL sample, a 0.07 m diameter circular GCL specimen was cut at the thin spot in sample N5 and the thickness of the GCL specimen was measured using a line laser. The thickness at the thin spot was 6.1 ± 0.2 mm (range: 5.6–6.5 mm), which was less than the average thickness of the GCL (6.9 ± 0.2 mm) outside the thin zone. Consistent with the visual inspection, X-ray images showed cracks in both GCL3 and GCL4 (Fig. 10).

The visual inspection of GCL1 and GCL2 suggested that, because of the dispersed and well-hydrated structure of the bentonite, they may be an effective hydraulic barrier after 7 years in the field. For GCL3 and GCL4 and for all GCLs at the thin and (or) cracked

Fig. 10. X-ray images for GCL4 exhumed after (*a*) 5 years and (*b*) 7 years.
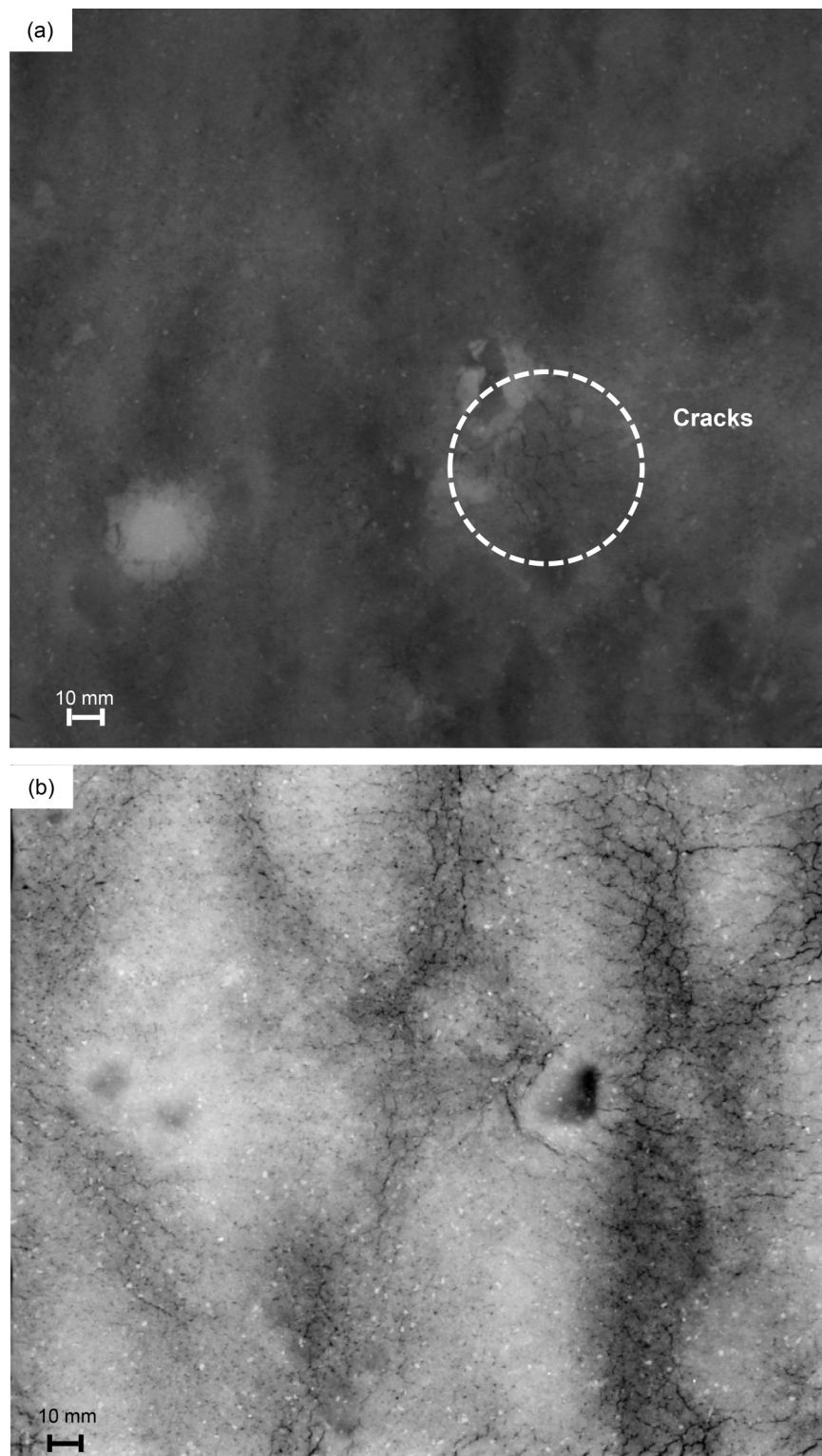
spots or where roots were penetrating vertically through the bentonite layer, questions arose as to how effective these GCLs (or portions thereof) would be as a hydraulic barrier. To provided quantitative insight into the performance of the GCLs after exposure, hydraulic conductivity tests were performed on both the "regular" GCLs (i.e., where there were no apparent defects) as well as the GCLs at the location of the various features discussed above.

Swell index and exchangeable cations

The initial SI of all GCLs examined was 24–26 mL/2 g (Table 7). GCL1 and GCL2 had a montmorillonite content of 96% (Table 1), an initial ESP of 67%–68%, and the exchangeable calcium percentage (ECP) was 23%–24%. GCL3 and GCL4 had a smectite content of 77%–84% (Table 1) and an initial ESP and ECP values of 80% and 13%, respectively. Accounting for the difference in montmorillon-

Table 7. Swell index and exchangeable cations of virgin and 5 year GCLs.

Sample	GCL type	Swell index (mL/2 g)	CEC (cmol/kg)[a]	Exchange complex (mole fraction)			
				Na[a]	K	Ca[b]	Mg[c]
Virgin GCL	GCL1	26±1	72±6	0.67±0.02	0.03±0.00	0.23±0.01	0.08±0.00
	GCL2	25±1	78±2	0.68±0.02	0.02±0.01	0.24±0.03	0.06±0.02
	GCL3	24±1	91±8	0.80	0.02	0.13	0.04
	GCL4	24±1	85±5	0.80	0.02	0.13	0.04
N1	GCL1	10 (SD = 1, n = 3)	90 (SD = 8, n = 2)	0.00	0.01	0.74	0.25
N2	GCL2	10 (SD = 0, n = 3)	92	0.05	0.04	0.68	0.22
N5	GCL2	11 (SD = 1, n = 3)	100	0.07	0.04	0.68	0.21
N6	GCL2	11 (SD = 1, n = 3)	92	0.07	0.04	0.68	0.21
N3	GCL3	8 (SD = 0, n = 3)	97	0.00	0.01	0.78	0.22
N4	GCL4	8 (SD = 0, n = 3)	78 (SD = 7, n = 2)	0.00	0.01	0.76	0.22

Note: Swell index and cation exchange capacity (CEC) carried out according to ASTM standards D5890-06 (ASTM 2006) and D7503-10 (ASTM 2010), respectively, except using air-dried bentonite for swell index test instead of using oven-dried bentonite as specified in ASTM D5890-06.

[a]Exchangeable sodium percentage.
[b]Exchangeable calcium percentage.
[c]Exchangeable magnesium percentage.

ite and initial ESP, all GCLs had about the same initial exchangeable sodium per gram.

After 5 years of exposure to the porewater of cover and foundation soil, the SI of GCL1 (sample N1) decreased to 10 mL/2 g (i.e., within the typical range of calcium bentonite; Mitchell 1993), because the Na$^+$ in the exchange sites (ESP = 0%) had been completely replaced by Ca^{2+} (ECP = 74%) and Mg^{2+} (the exchangeable magnesium percentage (EMP) increased from 8% to 25%). Similarly, the three samples (N2, N5, and N6) exhumed from the GCL2 panel had almost the same chemical characteristics with a measured SI of 10–11 mL/2 g and ESP of 5%–7%, which coincided with an increase in the ECP and EMP to 68% and 21%–22%, respectively. The reduction in SI and ESP of the 7 year samples was similar to these measured for the 5 year samples. Despite this reduction in the swelling capacity of the bentonite of GCL1 and GCL2, no cracks were observed by visual inspection or X-ray suggesting that the consolidation or compression induced by the 0.7 m overburden either prevented any cracks from developing or visually healed any that had been formed when the GCL was exposed to moisture movement due to seasonal wet–dry cycles over the 7 years of exposure.

On the other hand, although the exhumed GCL3 and GCL4 samples had similar SI (8 mL/2 g) and ESP (0%) values to GCL1 and GCL2, indicating similar total cation exchange between monovalent cation in GCLs with divalent cations in soil porewater, there was a difference in the bentonite structure where cracks or macrovoids between granules were observed at some locations in GCL3 and GCL4. These cracks or macrovoids appeared to be associated with the initial coarse granular bentonite in GCL3 and GCL4, which had to swell more than the fine granular bentonite in GCL1 and GCL2 to close the bigger initial macropores of GCL3 and GCL4.

Hydraulic conductivity

Performance of GCL1

The k value of virgin GCL1 hydrated and permeated with 10 mmol/L CaCl$_2$ solution under 1.2 m differential head and 15 kPa effective stress was 3.8 × 10^{-11} m/s. When triplicate regular exhumed specimens from sample N1 (5 year sample; M_b = 5200–5500 g/m^2, thickness = 7.5–7.9 mm) were permeated with 10 mmol/L CaCl$_2$ solution, the k values varied between 4.0 × 10^{-11} and 2.2 × 10^{-10} m/s (depending on the specimen) under a differential head (ΔH) across the GCL specimens of 0.07–1.2 m (Table 3 and Fig. 11). For duplicate regular 7 year specimens extracted from sample NA, k values (1.4 × 10^{-10} to 4.1 × 10^{-10} m/s) were similar to that measured for the regular 5 year specimens under ΔH of 0.07–1.2 m.

For a "thin" GCL1 specimen (M_b = 4600 g/m^2, thickness = 5 mm) exhumed from sample N1, there was a very little difference in the

Fig. 11. Hydraulic conductivity of GCL1 specimens versus the head across the GCL when tested in FWPs for samples exhumed after 5 and 7 years. Horizontal bars represent range of permeant head across GCL under falling-head test condition in FWPs. Hydraulic conductivity values presented are mean and vertical error bars are range of measured k when multiple tests carried out.
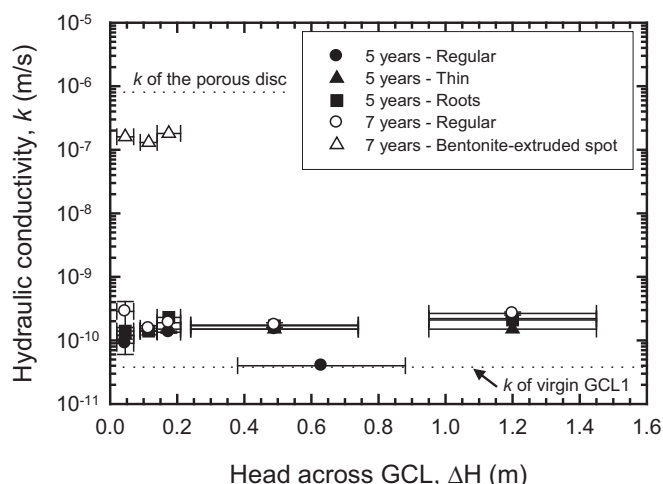
measured k values (1.2–1.5 × 10^{-10} m/s) compared to regular specimens under the range of heads of 0.07–1.2 m. Similarly, the measured k values for a GCL1 specimen with roots penetrating vertically through the GCL were in the range of 1.4 × 10^{-10} to 2.3 × 10^{-10} m/s under ΔH of 0.07–1.2 m. Thus, despite the complete replacement of Na$^+$ in the bentonite of GCL1 by Ca^{2+} and Mg^{2+}, k for all tested specimens from GCL1 only increased by a factor of 10 after 7 years in service at the site with no significant change in k when ΔH increased from 0.07 to 1.2 m. These low k values were consistent with the well-hydrated bentonite structure seen in the X-ray images for GCL1 (Fig. 8). The only exception for the low measured k values was for the GCL specimen extracted from GCL1 where bentonite extrusion took place (Figs. 8b and 12). There was a decrease in the area of the extruded part of the GCL with the extruded bentonite upon hydration and permeation and the area of the bentonite extruded spot in the tested GCL1 specimen decreased due to permeation under loading from 18 mm × 8 mm (Fig. 12a) to 13 mm × 6 mm after k testing (Fig. 12b). However, the bentonite extruded spot after permeating and loading in FWP was still large enough to cause high leakage through the tested spec-

Fig. 12. X-ray photos for 7 year GCL1 specimen with a bentonite extrusion spot (see Fig. 8b) (a) directly after exhumation before any k test and (b) after permeation in FWP using 10 mmol/L CaCl$_2$ solution under 15 kPa stress.
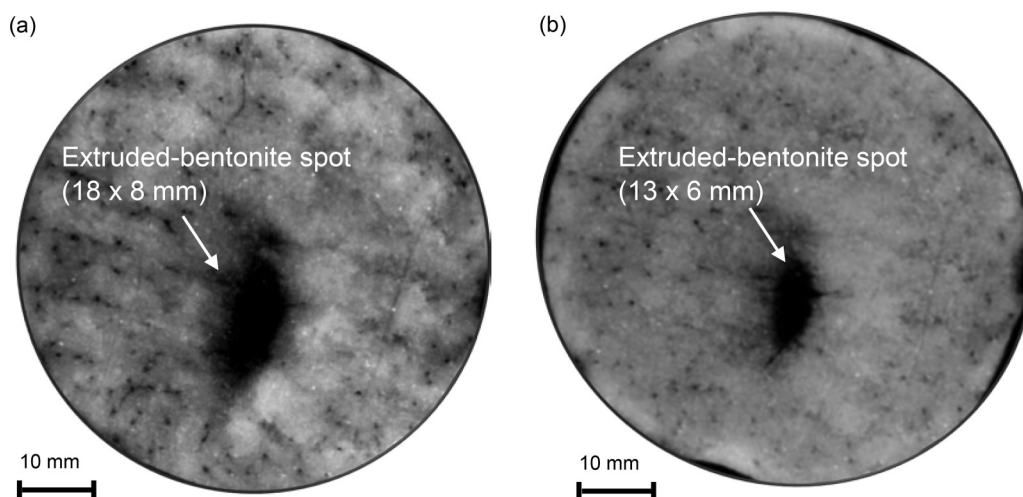
Fig. 13. (a) Carrier GTX of GCL1 specimen (outflow side), (b) cover GTX of GCL1 specimen (inflow side), and (c) view along cross section A–A for GCL1 specimen at end of k test in FWPs (bentonite in (c) was partially removed to expose bundles). [Colour online.]
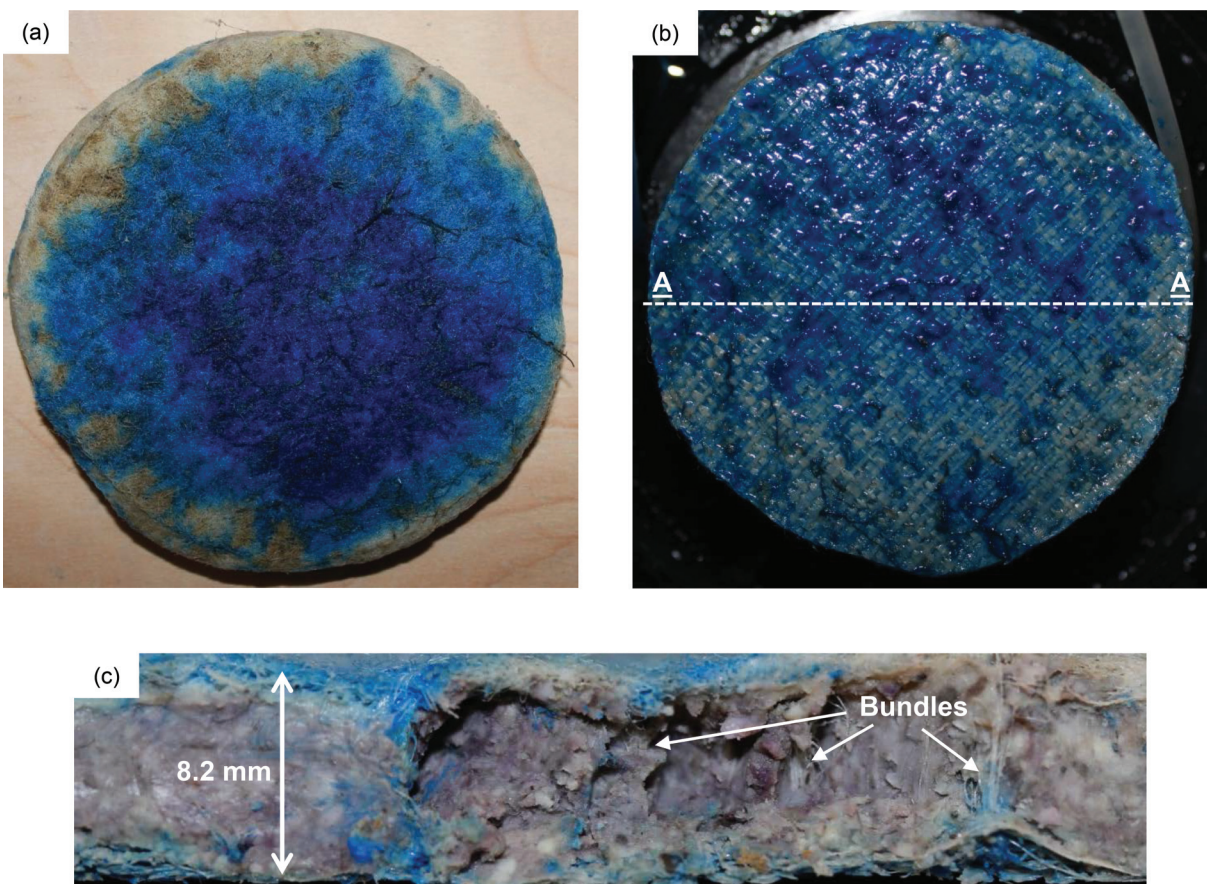
imen (equivalent k of 1.3×10^{-7} to 1.8×10^{-7} m/s under a head of 0.07–0.21 m; Fig. 11).

The k value of the porous discs used in the FWP above and below the tested GCL specimens was 8×10^{-7} m/s (drawn as a horizontal dotted line in Fig. 11). According to the ASTM (2008b) standard D5887, k of the porous discs should be at least 1 order of magnitude higher than k of the tested specimen; a condition satisfied for all tested GCL1 specimens. Because the Na$^+$ in all exhumed GCL samples was completely replaced by divalent cations, no further cation exchange was expected between the permeant and the bentonite during k tests and equilibrium was reached once the inflow and outflow attained the same constant value.

At the end of each k test and before termination, the tested specimens were permeated with blue dye–spiked 10 mmol/L CaCl$_2$ solution. The flow through all GCL1 specimens was typically uniformly distributed over the GTX in the outflow side (Fig. 13a) and

Fig. 14. (*a*) Hydraulic conductivity of GCL2 specimens versus head across GCL when tested in FWPs for samples exhumed after 5 and 7 years. Horizontal bars represent range of permeant head across GCL under falling-head test condition in FWPs. Hydraulic conductivity values presented are mean and vertical error bars are range of measured *k* when multiple tests carried out. (*b*) Cross section of GCL2 regular specimen after *k* test in FWP (bentonite was partially removed to expose bundles). [Colour online.]
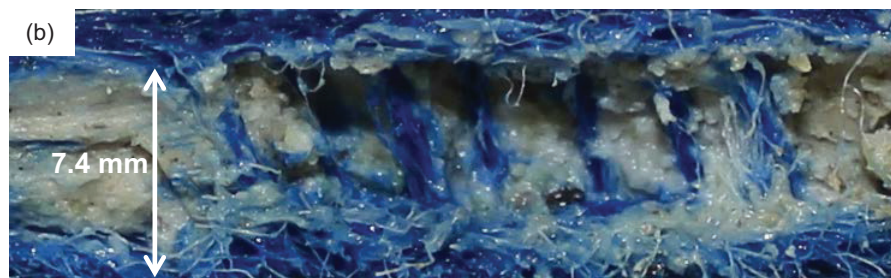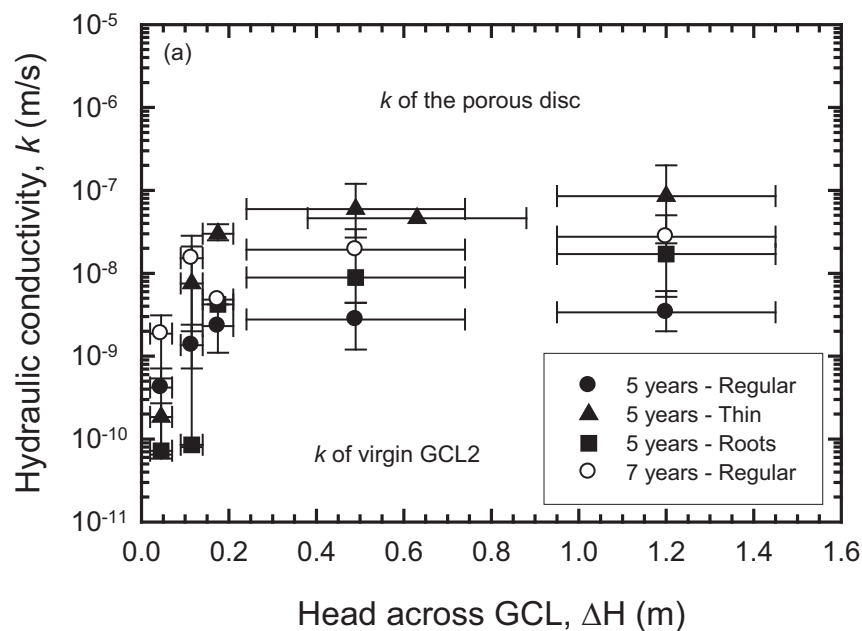
the inflow side (Fig. 13*b*). In addition, the flow was uniformly distributed within the bentonite layer (Fig. 13*c*) with no observed preferential flow path either within the bentonite structure or the needle-punched fibres.

When a regular GCL1 specimen was tested in the FWP under 0.07 m head and 15 kPa effective stress using different permeants, there was no change in *k* (8.4×10^{-11} to 8.6×10^{-11} m/s) with the increase in calcium concentration in the permeant from 40 mg/L (tap water) to 400 mg/L (10 mM $CaCl_2$ solution). This was expected as there was no cation exchange expected to take place between the bentonite and the permeant given the exchange that had already taken place in the field.

In summary, *k* of all tested GCL1 specimens was in the range of 4×10^{-11} to 4.1×10^{-10} m/s when permeated with 1–10 mmol/L $CaCl_2$ solution under ΔH of 0.07–1.2 m with the value at low head (ΔH = 0.07 m) being 6.0×10^{-11} to 1.4×10^{-10} m/s. There was no significant effect of ΔH in the measured *k* values. There was no preferential flow through the bentonite or needle-punched bundles of tested specimens.

Performance of GCL2

The *k* of virgin GCL2 was 4.4×10^{-11} m/s when permeated with 10 mmol/L $CaCl_2$ solution under ΔH of 1.2 m and 15 kPa effective stress. Because there was no significant difference in the chemical and hydraulic performance of samples N2, N5, and N6 exhumed from the GCL2 panel (e.g., see Table 7), *k*-tested specimens with

similar bentonite structure and M_b from the three exhumed samples were considered identical and presented in the same graph (Fig. 14 and Table 4). The *k* values of triplicate 5 year regular GCL2 specimens (M_b = 5300–6000 g/m², thickness = 7.4–9.1 mm) tested in FWPs under 0.07 m head (effective inflow, outflow, and average stress values were 14.5, 15.2, and 15 kPa, respectively) varied between 6.5×10^{-11} and 7.1×10^{-10} m/s (average of 4.2×10^{-10} m/s). The *k* value of regular 7 year GCL2 specimen (5.4×10^{-10} m/s) was similar to the *k* values measured for the 5 year regular specimens. This measured *k* value represents an increase in average *k* (relative to virgin) by about 1 order of magnitude; however, in many liner applications this *k* value would be adequate to maintain low leakage. When ΔH was increased to 0.14 m (effective inflow, outflow, and average stress values were 13.8, 15.2, and 15 kPa, respectively), there was an increase in *k* of the 5 and 7 year specimens to an average of 1.4×10^{-9} m/s (*k* values of the four tested specimens at 0.14 m were 8.0×10^{-11}, 1.6×10^{-9}, 2.0×10^{-9}, and 2.4×10^{-9} m/s; Table 4). Although there was an increase in the average *k* value by a factor of 3 when the head increased from 0.07 to 0.14 m (Fig. 14), the two sets of *k* values under both heads overlapped with each other and were statistically similar (at a 95% confidence level). For ΔH of 0.21–1.2 m (for ΔH of 0.21, 0.49, and 1.2, the effective inflow stress values were 13.8, 12.4, and 8.9 kPa, respectively, where the effective outflow stress values were 15.9, 17.3, and 20.7 kPa, respectively), the *k* values were 2.0–6.1×10^{-9} m/s, which is 5–8 times the

Fig. 15. Variation in hydraulic conductivity of GCL2 with (*a*) dry bentonite mass per unit area and (*b*) GCL thickness under $\Delta H = 1.2$ m.
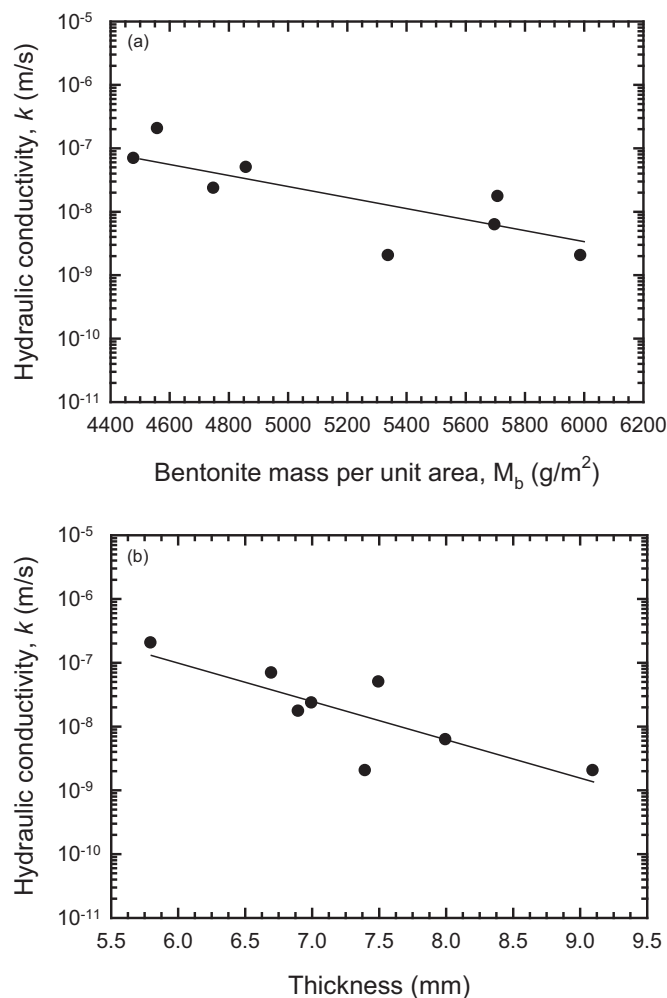
k values measured at 0.07 m and about 2 orders of magnitude higher than *k* of virgin GCL2. Thus, for regular 5 and 7 year GCL2 specimens, there was an increase in *k* by about 1 order of magnitude when the differential head across the GCL was 0.07–0.14 m, while the increase in *k* was by about 2 orders of magnitude when the head was 0.21–1.2 m, both relative to virgin specimens.

The *k* value of a 5 year GCL2 specimen with roots penetrating vertically through the GCL ($M_b = 5700$ g/m², thickness = 6.9 mm) was similar to samples with no roots (regular specimens) when the head was ≤0.14 m. When the head increased to 0.21–1.2 m, there was an increase in *k* (4.2×10^{-9} to 1.7×10^{-8} m/s) for a specimen with roots by a factor of 3–5 compared to specimens with no roots (2.0×10^{-9} to 6.1×10^{-9} m/s).

The average *k* values of five thin 5 year GCL2 specimens and one thin 7 year specimen ($M_b = 4300$–4900 g/m², thickness = 5.8–7.3 mm) tested in FWPs under ΔH of 0.07 m (average $k = 7.8 \times 10^{-10}$ m/s; varied between 5.8×10^{-11} and 3.2×10^{-9} m/s) and 0.14 m (average $k = 1 \times 10^{-8}$ m/s; varied between 7.1×10^{-10} and 2.8×10^{-8} m/s) were in the same range of the *k* values measured for the regular specimens. However, with the increase in head to 0.21–1.2 m, the *k* value of the thin specimens ($k = 6.8 \times 10^{-8}$ to 2.0×10^{-7} m/s) was about 1–2 orders of magnitude higher than the *k* values of regular specimens. Thus, the *k* values for GCL2 were sensitive to both M_b and ΔH (regular versus thin specimens). Figures 15*a* and 15*b* show the correlation between measured *k*

values for regular and thin specimens (under $\Delta H = 1.2$ m) with variation of GCL M_b and thickness, respectively.

Unlike GCL1, the flow through all GCL2 specimens (regular and thin) tested under relatively high hydraulic gradients occurred mainly through the bundles (Fig. 14*b*). This difference in the flow pattern between GCL1 (Fig. 13*c*) and GCL2 (Fig. 14*b*) specimens may be attributed to the difference in the size of bundles and the percentage area covered by the bundles (Table 2). Based on the change in *k* of GCL2 with head (Fig. 14*a*) and the flow pattern for GCL2 specimens (Fig. 14*b*), it appears that under a head of 0.07 m the bentonite was sealing and filling the 1.1 mm diameter bundles and the measured increase in *k* of GCL2 under ΔH of 0.07 m by ≤1 order of magnitude was a result of the loss of the exchangeable Na⁺ during cation exchange with the subgrade in the field. Thus, this *k* represents the *k* of the bentonite after cation exchange for the conditions examined. When the head increased to 0.14 m, the bentonite began to be less effective at sealing around the bundles (it is speculated that this may be because bentonite began to be eroded out from the bundles) and *k* increased on average. At heads ≥0.21 m, it may be hypothesized that internal erosion and (or) particle movement or re-orientation of the bentonite took place around and at the bundles, which allowed preferential flow at or through the bundles and as a result, *k* increased by 2–4 orders of magnitude depending on M_b and the thickness of the GCL, with thicker specimens and more bentonite surrounding the bundles increasing the resistance to preferential flow. In contrast, the increase in head across GCL1 specimens for up to 1.2 m apparently did not cause change in the bentonite structure at or around the bundles, because the size of bundles and percentage area covered by bundles in GCL1 were smaller than those for GCL2, making it more difficult for the permeant to wash out the bentonite from the relatively small bundles.

To test the aforementioned hypothesis, regular GCL2 specimens were tested under a constant head of 0.07 m. The *k* values (5.5×10^{-11} to 9.7×10^{-11} m/s) under ΔH of 0.07 m were not affected by the permeant for 1, 5, and 10 mmol/L CaCl₂ solutions (Fig. 16*a*) and the flow occurred through the bentonite (Fig. 16*b*) with no preferential flow through the needle-punched fibres. The difference in the flow pattern between GCL2 specimens tested under high ΔH (1.2 m) and low ΔH (0.07 m) supports the hypothesis presented earlier regarding the effect of water head in causing change(s) in the bentonite structure or movement of clay particles, especially at bundle locations.

In summary, *k* of GCL2 under low ΔH (0.07 m) was relatively low (7×10^{-11} to 4×10^{-10} m/s) for all tested specimens (regular, thin or with roots penetrating the GCL). Between a head of 0.07 and 0.21 m (depending on the M_b), there was particle movement or structural change of the bentonite, most likely at needle-punched bundles, which caused an increase in average *k*. Under ΔH of 1.2 m, *k* increased by 2–4 orders of magnitude (relative to virgin value) to 2.0×10^{-9} to 2.0×10^{-7} m/s, with the actual value depending on M_b.

Performance of GCL3 and GCL4

The *k* value of the 5 and 7 year GCL3 specimens (GCL with coarse granular bentonite and needle-punch bundle size of 1.2 mm) permeated in the FWPs with the 10 mmol/L CaCl₂ solution (Table 5 and Fig. 17) depends mainly on the applied head. When there were no visible cracks in the bentonite (regular specimens with $M_b = 5200$–5600 g/m², thickness = 7.8–8.4 mm), the *k* values under ΔH of 0.07 m varied between 7.6×10^{-11} and 7.0×10^{-10} m/s. When roots were penetrating vertically through a GCL3 specimen with $M_b = 5800$ g/m² (thickness = 9 mm), *k* ($\Delta H = 0.07$ m) was 2.7×10^{-10} m/s. For a specimen with cracked bentonite, *k* ($\Delta H = 0.07$ m) was 6.3×10^{-10} m/s. Despite this increase in *k* under 0.07 m head compared to virgin GCL3, it may still be considered low enough for many practical applications. Between a head of 0.07 and 0.14 m, particle movement or structural change of bentonite at or around the bundles occurred and as a result the *k* value increased

Fig. 16. (*a*) Hydraulic conductivity of GCL2 regular specimens tested in the FWPs under 0.07 m head across specimen with different permeants (values presented are mean and range). (*b*) Cross section of tested GCL specimen after termination (bentonite was partially removed to expose bundles). [Colour online.]
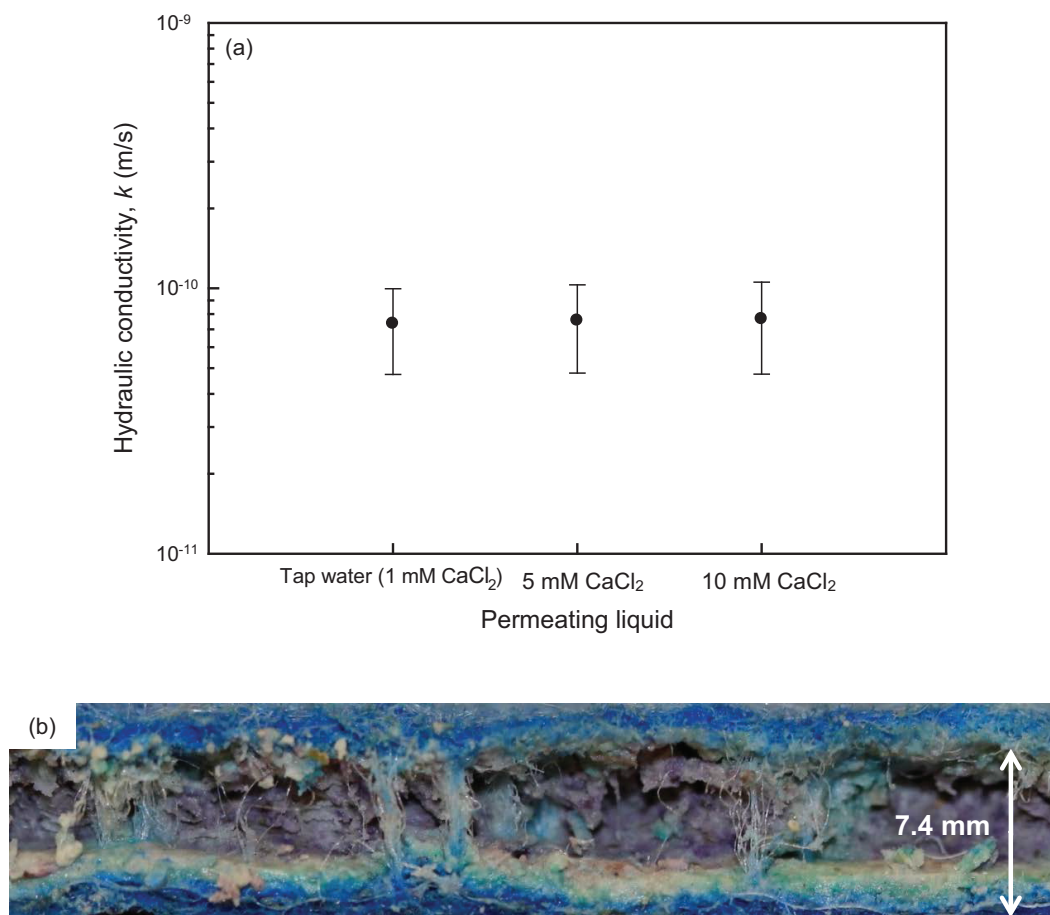
by 3–4 orders of magnitude to be in the range of 3.0×10^{-9} to 6.0×10^{-8} m/s. Once the particle movement or structural change of bentonite took place, the bentonite layer seemed to have no effect on k because of preferential flow through the needle-punch bundles (Fig. 17*b*). For $\Delta H = 0.14$–1.2 m, k of all tested GCL3 specimens was in the range of 4.1×10^{-9} to 7.3×10^{-8} m/s.

The hydraulic performance of the other GCL product with coarse granular bentonite (GCL4; Fig. 18*a*) was similar to that for GCL3 although the k value under $\Delta H > 0.07$ m for GCL4 was almost double that of GCL3. This may be because of the difference in bundle size (1.6 mm for GCL4 versus 1.2 mm for GCL3) and percentage area covered by bundles (14% for GCL4 versus 9% for GCL3). When $\Delta H = 0.07$ m (Table 6 and Fig. 18*a*), the k values were 9.3×10^{-11} (average of four specimens at 5 and 7 years), 3.9×10^{-9}, and 1.3×10^{-9} for regular, cracked, and with roots specimens, respectively. Similar to GCL3, the particle movement or structural change of bentonite at or around the bundles took place when the head was 0.07–0.14 m. The k values increased to 1–2×10^{-7} m/s for ΔH of 0.21–1.2 m and the flow was concentrated within the bundles (Fig. 18*b*).

Correlation between hydraulic conductivity and properties of bundles and practical implications

Based on all tested GCLs, a correlation between the measured k values at 1.2 m head and the percent area covered by bundles (Fig. 19*a*) and size of bundles (Fig. 19*b*) showed that the final k value of a GCL under 1.2 m head (gradient of 120–170) is highly dependent on the characteristics of the bundles. The most important observations from the k tests reported herein is that the (*i*) hydrau-

lic head across the GCL, (*ii*) properties of the needle-punched bundles (i.e., size of bundles and percentage area covered by bundles), and (*iii*) bentonite structure can all significantly affect the value of k measured for low-stress field-exposed GCLs.

The very important implications of the foregoing for those conducting laboratory tests for the hydraulic performance of GCL samples exhumed from the field after exposure to significant cation exchange is that the use of a gradient (ΔH / GCL thickness) greater than that expected in the field may substantially overestimate the k values. The larger the size of the bundles, the higher the likelihood of the particle movement or structural change of bentonite at or around the bundles that will cause a preferential flow for liquids to occur. Based on the GCLs tested herein, no particle movement or structural change of bentonite at or around the bundles was detected for GCL products with fine granular bentonite with an average bundle size ≤0.7 mm and 4% area covered by bundles, even when the sodium in the GCL was completely replaced by divalent cations (k was 1.5–2.2×10^{-10} m/s at $\Delta H = 1.2$ m). For GCLs with fine granular bentonite and an average bundles size of 1.1 mm and 9% area covered by bundles and GCLs with coarse granular bentonite with average bundles = 1.2–1.6 mm and 9%–14% area covered by bundles, k was also governed by the effect of cation exchange on the bentonite (and not the needle punching) under low head across the GCL (0.07 m). However, for these three GCLs the needle-punched bundles dominated the flow and gave rise to a sudden large increase in k for $\Delta H > 0.2$ m.

Generally, there is an impression that higher peel strength is better than lower peel strength. Certainly that is true when high

Fig. 17. (*a*) Hydraulic conductivity of GCL3 specimens versus head across GCL when tested in FWPs for samples exhumed after 5 and 7 years. Horizontal bars represent range of permeant head across the GCL under falling-head test condition in FWPs. Hydraulic conductivity values presented are mean and vertical error bars are range of measured k when multiple tests carried out. (*b*) Cross section of GCL3 regular specimen after k test in FWP (bentonite was partially removed to expose bundles). [Colour online.]
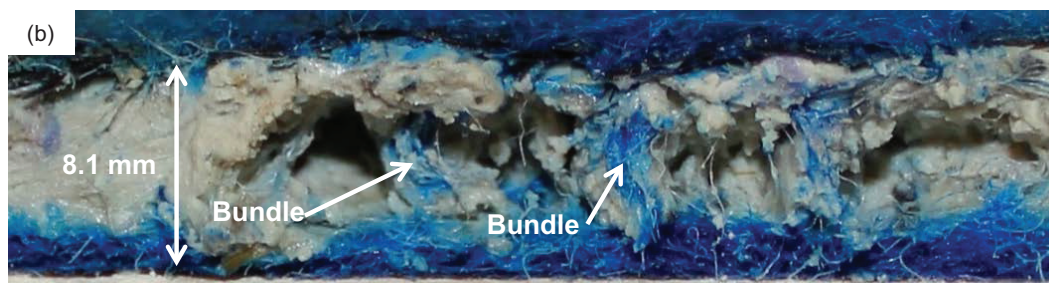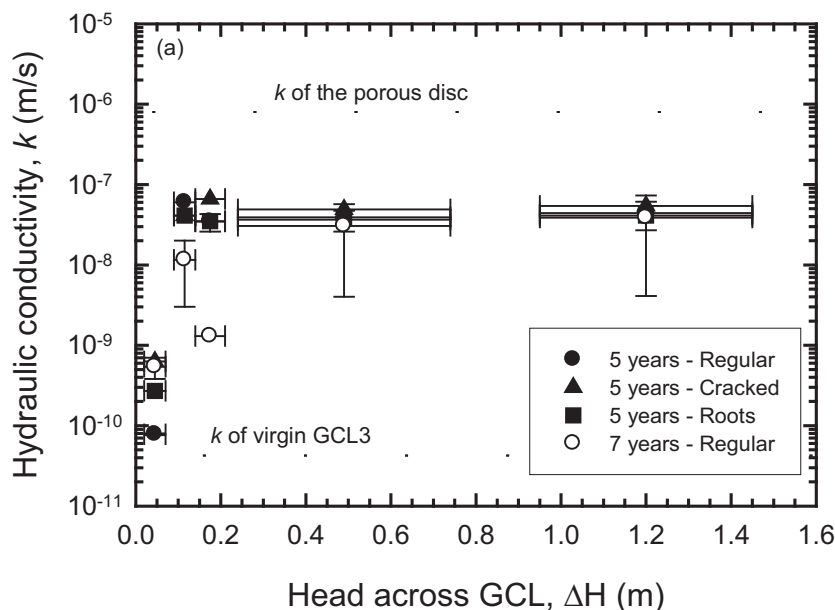
interface shear is required. However, for the designer, the forgoing also implies that if the GCL will be covered in a timely manner by a suitable thickness of cover soil, then the peel strength should not be more than required to ensure internal stability. Excessive needling will decrease the hydraulic performance of the GCL serving under low stress following cation exchange for $\Delta H > 0.2$ m.

While one GCL performed better than the other three GCLs at $\Delta H > 0.2$ m, it is important to recognize that this is the result for the rolls tested and may not be true for other rolls from the plant, because the needling may vary depending on a number of factors including the wear of the needles. The four products tested have a stated minimum peel strength (ASTM (2015) standard D4632) of 93 N (GCL1 and GCL2; Table 2) and 95 N (GCL3 and GCL4). GCL1 had needling that gave an average peel of 94 N, which just meets the manufacturer's minimum. GCL2 had a peel strength of 261 N (i.e., 2.8 times the stated product minimum). GCL3 and GCL4 had average peel strengths of 204 and 219 N, respectively (i.e., 2.1–2.3 times the minimum). The extra needling that gave rise to these high peel strengths (more than twice the minimum) was also responsible for the poor hydraulic performance of the GCLs for $\Delta H > 0.2$ m.

Finally, the GCLs examined had fine and coarse bentonite. There was an observed difference in the hydration of the two types. The fine bentonite had hydrated to a gel while the coarse bentonite had been partially hydrated with macrovoids between

the larger granules that had not hydrated significantly. It is not known how a GCL with powdered bentonite would perform under similar conditions and especially whether the response after cation exchange would be similar to or different from that reported herein for the GCLs examined.

Summary and conclusions

A 20 m wide × 76 m long simulated landfill cover comprising a layer of four different needle-punched GCL products with granular Wyoming sodium bentonite covered by 0.7 m of silty sand was constructed at Godfrey (north of Kingston), Ontario, Canada, in the summer of 2006. Five and 7 years after construction, GCL panels were exposed at different locations and the physical performance of the GCL overlaps was inspected. In addition, GCL samples were exhumed from the four products to assess the bentonite structure, chemical characteristics of bentonite (mainly swell index and exchangeable cations), and the hydraulic conductivity of GCLs. The following conclusions were reached for the specific materials and conditions examined after up to 7 years of exposure in the test cover:

1. The 300 mm GCL overlaps with 0.4 kg/m supplemental bentonite were physically intact with a horizontal and downward separation between panels of <8 mm and <35 mm, respec-

Fig. 18. (a) Hydraulic conductivity of GCL4 specimens versus head across GCL when tested in FWPs for samples exhumed after 5 and 7 years. Horizontal bars represent range of permeant head across the GCL under falling-head test condition in FWPs. Hydraulic conductivity values presented are mean and vertical error bars are range of measured k when multiple tests carried out. (b) Cross section of GCL4 regular specimen after k test in FWP (bentonite was partially removed to expose bundles). [Colour online.]
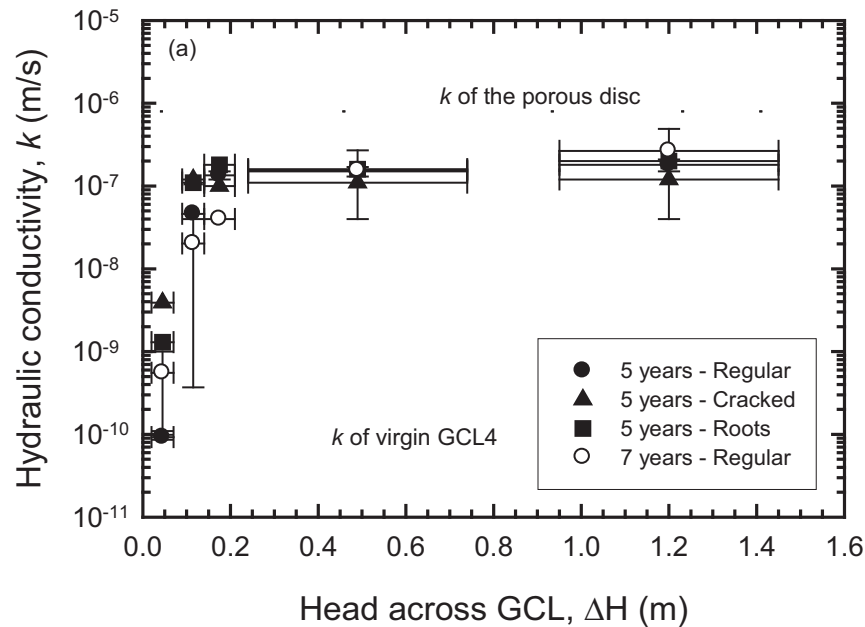
tively. In addition, the supplemental bentonite was well hydrated and there was no evidence of any negative impacts on the hydraulic performance of the overlaps.

2. The bentonite in GCL products with fine granular bentonite ($53\% < W_c < 77\%$; $0.50 < W_c/W_{ref} < 0.74$) visually appeared as well-hydrated gel with no visible defects in the GCL components. However, there were occasional thinner bentonite areas caused by irregularities (small stones or soil clods) in the foundation layer. Despite the similarity in water content with the GCL having fine-grained bentonite, the bentonite in GCL products with coarse granular bentonite ($63\% < W_c < 77\%$; $0.44 < W_c/W_{ref} < 0.60$) did not look well hydrated at some locations and cracks in the bentonite layer were observed in X-ray images of these samples. Thus, the initial particle size of the bentonite appears to make a difference in the bentonite structure at the water contents at which they were exhumed in the field after 7 years of exposure.

3. The sodium in all exhumed GCL samples was essentially completely replaced by calcium and magnesium and the measured swell index was 8–11 mL/2 g and an exchangeable sodium percentage 0%–7% for all samples.

4. The k value of GCL1 specimens (with fine granular bentonite and an average bundle size of 0.7 mm) permeated with 10 mmol/L CaCl$_2$ solution was low at 4×10^{-11} to 4.1×10^{-10} m/s

under an applied head difference of 0.07–1.2 m and 15 kPa effective stress. The increase in k was solely due to the effect of cation exchange on the bentonite and there was no effect for the applied water head (over the range examined) on the measured k values. The flow of the permeant was distributed uniformly through the bentonite layer.

5. At low head ($\Delta H = 0.07$ m), GCL2 (with fine granular bentonite and average bundle size of 1.1 mm) maintained low hydraulic conductivity. However, at a head between 0.07 and 0.21 m, the bentonite ceased to seal effectively around the bundles and there was preferential flow that started to occur through the bundles causing an increase in k of 2–4 orders of magnitude (relative to virgin GCL) depending on the mass of bentonite.

6. The k value of GCLs with coarse granular bentonite and an average bundle size of 1.2–1.6 mm was in the range of 7.6×10^{-11} m/s (specimen without cracks) to 3.9×10^{-9} m/s (specimen with cracks) when the applied head was 0.07 m. At an applied head between 0.07 and 0.14 m, particle movement or structural change of bentonite at or around the bundles took place and k increased to 2×10^{-8} to 2×10^{-7} m/s.

7. The hydraulic head across the GCL and the properties of the needle-punched bundles (i.e., percentage area covered by bundles and size of bundles) greatly affect the measured k

Fig. 19. Hydraulic conductivity of regular 5 and 7 year GCLs tested under applied head of 1.2 m and with 10 mmol/L $CaCl_2$ solution as permeant versus (*a*) percent area covered by bundles and (*b*) average and maximum measured bundle sizes.

carefully inspected or checked by the authors who were on site throughout construction. The experimental site was constructed on a property owned by Cruickshank Construction Ltd., who also conducted the associated earthworks. The use of their property and assistance during construction are greatly appreciated. There was no oversight or role played by any of those acknowledged above, or anyone else other than the authors, in any portion of the study design or in the collection, analysis, and interpretation of data, nor in the writing of this paper and the decision to submit it for publication. The authors accept full responsibility for the data and any interpretation or statements made in the paper. The contributions of L.E. Bostwick and R. Beddoe and M. Chappel with the construction of the field site in 2006 is gratefully acknowledged.

References

ASTM. 2004. Standard test methods for measurement of hydraulic conductivity of saturated porous materials using a flexible wall permeameter. ASTM standard D5084-03. American Society for Testing and Materials. doi:10.1520/D5084-03.

ASTM. 2006. Standard test method for swell index of clay mineral component of geosynthetic clay liners. ASTM standard D5890-06. American Society for Testing and Materials. doi:10.1520/D5890-06.

ASTM. 2008*a*. Standard practice for obtaining samples of geosynthetic clay liners. ASTM standard D6072-08. American Society for Testing and Materials. doi:10.1520/D6072-08.

ASTM. 2008*b*. Standard test method for measurement of index flux through saturated geosynthetic clay liner specimens using a flexible wall permeameter. ASTM standard D5887-08. American Society for Testing and Materials. doi:10.1520/D5887-08.

ASTM. 2010. Standard test method for measuring the exchangeable complex and cation exchange capacity of inorganic fine-grained soils. ASTM standard D7503-10. American Society for Testing and Materials. doi:10.1520/D7503-10.

ASTM. 2015. Standard test method for grab breaking load and elongation of geotextiles. ASTM standard 4632-15a. American Society for Testing and Materials. doi:10.1520/D4632_D4632M-15A.

Bathurst, R.J., Rowe, R.K., Zeeb, B., and Reimer, K. 2006. A geocomposite barrier for hydrocarbon containment in the Arctic. International Journal of Geo-engineering Case Histories, **1**(1): 18–34.

Benson, C.H., and Meer, S.R. 2009. Relative abundance of monovalent and divalent cations and the impact of desiccation on geosynthetic clay liners. Journal of Geotechnical and Geoenvironmental Engineering, **135**(3): 349–358. doi:10.1061/(ASCE)1090-0241(2009)135:3(349).

Benson, C., Thorstad, P., Jo, H., and Rock, S. 2007. Hydraulic performance of geosynthetic clay liners in a landfill final cover. Journal of Geotechnical and Geoenvironmental Engineering, **133**(7): 814–827. doi:10.1061/(ASCE)1090-0241(2007)133:7(814).

Benson, C., Kucukkirca, E., and Scalia, J. 2010. Properties of geosynthetics exhumed from a final cover at a solid waste landfill. Geotextiles and Geomembranes, **28**(6): 536–546. doi:10.1016/j.geotexmem.2010.03.001.

Boardman, B., and Daniel, D. 1996. Hydraulic conductivity of desiccated geosynthetic clay liners. Journal of Geotechnical and Geoenvironmental Engineering, **122**(3): 204–208. doi:10.1061/(ASCE)0733-9410(1996)122:3(204).

Bouazza, A., Van Impe, W.F., and Van Den Broeck, M. 1996. Hydraulic conductivity of a geosynthetic clay liner under various conditions. *In* Procedings of the 2nd International Congress on Environmental Geotechnics, Osaka, Japan. Vol. 1, pp. 453–458.

Bouazza, A., Jefferis, S., and Vangpaisal, T. 2007. Investigation of the effects and degree of calcium exchange on the Atterberg limits and swelling of geosynthetic clay liners when subjected to wet–dry cycles. Geotextiles and Geomembranes, **25**(3): 170–185. doi:10.1016/j.geotexmem.2006.11.001.

Brachman, R.W.I., Rowe, R.K., Take, W.A., Arnepalli, D.N., Chappel, M., Bostwick, L.E., and Beddoe, R. 2007. Queen's composite geosynthetic liner experimental site. *In* Proceedings of the 2007 Canadian Geotechnical Conference, Ottawa, Ont. pp. 2135–2142.

Bradshaw, S.L., Benson, C.H., and Scalia, J. 2013. Hydration and cation exchange during subgrade hydration and effect on hydraulic conductivity of geosynthetic clay liners. Journal of Geotechnical and Geoenvironmental Engineering, **139**(4): 526–538. doi:10.1061/(ASCE)GT.1943-5606.0000793.

Bradshaw, S.L., Benson, C.H., and Rauen, T.L. 2016. Hydraulic conductivity of geosynthetic clay liners to recirculated municipal solid waste leachates. Journal of Geotechnical and Geoenvironmental Engineering, **142**(2): 04015074. doi:10.1061/(ASCE)GT.1943-5606.0001387.

Brown, L.C., and Shackelford, C.D. 2007. Hydraulic conductivity of a geosynthetic clay liner to a simulated animal waste solution. Transactions of the American Society of Agricultural and Biological Engineers, **50**(3): 831–841. doi:10.13031/2013.23148.

Buckley, J., Gates, W.P., and Gibbs, D.T. 2012. Forensic examination of field GCL performance in landfill capping and mining containment applications. Geotextiles and Geomembranes, **33**: 7–14. doi:10.1016/j.geotexmem.2012.02.006.

Canadian Geotechnical Society. 2006. Canadian foundation engineering manual (CFEM). 4th ed.

values of field-exhumed GCLs after being subjected to significant cation exchange.

8. Testing exhumed GCLs under hydraulic gradients higher than that expected in the field may yield substantially overestimated *k* values and misleading conclusions when there are significant needle-punched bundles and cation exchange.

Finally, with proper design (e.g., installing a drainage layer above the GCL to maintain low head above the GCL, and covering the GCL with enough soil to keep it away from weathering conditions), and selection of GCL type (GCL with a small enough bundle size and percent area of bundles that still provides sufficient strength), GCLs can act as an effective barrier in low stress applications (such as a cover system) even after complete cation exchange between sodium in the GCL and divalent cations in the surrounding soil.

Didier, G., Al Nassar, M., Plagne, V., and Cazaux, D. 2000. Evaluation of self healing ability of geosynthetic clay liners. *In* Proceedings of the International Conference on Geotechnical and Geological Engineering, Melbourne. [CD-ROM]. Technomic Press, Lancaster, Pa.

Environment Canada. 2013. National climate data and information archive. Available from http://climate.weather.gc.ca/climate_normals/results_e.html?stnID=4242&lang=e&dCode=0&province=ONT&provBut=Go&month1=0&month2=12 [accessed 16 November 2013].

Gu, B.X., Wang, L.M., Minc, L.D., and Ewing, R.C. 2001. Temperature effects on the radiation stability and ion exchange capacity of smectites. Journal of Nuclear Materials, **297**: 345–354. doi:10.1016/S0022-3115(01)00631-6.

Hosney, M.S., and Rowe, R.K. 2013. Changes in geosynthetic clay liner (GCL) properties after 2 years in a cover over arsenic-rich tailings. Canadian Geotechnical Journal, **50**(3): 326–342. doi:10.1139/cgj-2012-0367.

James, A., Fullerton, D., and Drake, R. 1997. Field performance of GCL under ion exchange conditions. Journal of Geotechnical and Geoenvironmental Engineering, **123**(10): 897–901. doi:10.1061/(ASCE)1090-0241(1997)123:10(897).

Jo, H.Y., Benson, C.H., Shackelford, C.D., Lee, J.M., and Edil, T.B. 2005. Long-term hydraulic conductivity of a geosynthetic clay liner (GCL) permeated with inorganic salt solutions. Journal of Geotechnical and Geoenvironmental Engineering, **131**(4): 405–417. doi:10.1061/(ASCE)1090-0241(2005)131:4(405).

Lange, K., Rowe, R.K., and Jamieson, H. 2010. The potential role of geosynthetic clay liners in mine water treatment systems. Geotextiles and Geomembranes, **28**: 199–205. doi:10.1016/j.geotexmem.2009.10.003.

Lee, J.M., Shackelford, C.D., Benson, C.H., Jo, H.Y., and Edil, T. 2005. Correlating index properties and hydraulic conductivity of geosynthetic clay liners. Journal of Geotechnical and Geoenvironmental Engineering, **131**(11): 1319–1329. doi:10.1061/(ASCE)1090-0241(2005)131:11(1319).

Lin, L., and Benson, C. 2000. Effect of wet-dry cycling on swelling and hydraulic conductivity of geosynthetic clay liners. Journal of Geotechnical and Geoenvironmental Engineering, **126**(1): 40–49. doi:10.1061/(ASCE)1090-0241(2000)126:1(40).

Mazzieri, F., Di Emidio, G., Fratalocchi, E., Di Sante, M., and Pasqualini, E. 2013. Permeation of two GCLs with an acidic metal-rich synthetic leachate. Geotextiles and Geomembranes, **40**: 1–11. doi:10.1016/j.geotexmem.2013.07.011.

McKnight, T.L., and Hess, D. 2000. Climate zones and types. *In* Physical geography: a landscape appreciation. Upper Saddle River, Prentice Hall, N.J.

Meer, S., and Benson, C. 2007. Hydraulic conductivity of geosynthetic clay liners exhumed from landfill final covers. Journal of Geotechnical and Geoenvironmental Engineering, **133**(5): 550–563. doi:10.1061/(ASCE)1090-0241(2007)133:5(550).

Melchior, S. 2002. Field studies and excavations of geosynthetic clay liner in landfill covers. *In* Clay geosynthetic barriers. *Edited by* H. Zanzinger, R.M. Koerner, and E. Gartung. A.A Balkema Publishers, Lisse. pp. 321–330.

Melchior, S., Sokollek, V., Berger, K., Vielhaber, B., and Steinert, B. 2010. Results from 18 years of in situ performance testing of landfill cover systems in Germany. Journal of Environmental Engineering, **136**(8): 815–823. doi:10.1061/(ASCE)EE.1943-7870.0000200.

Mitchell, J.K. 1993. Fundamentals of soil behavior. 2nd ed. John Wiley and Son, Inc., New York.

Petrov, R.J., and Rowe, R.K. 1997. Geosynthetic clay liner (GCL) – chemical compatibility by hydraulic conductivity testing and factors impacting its performance. Canadian Geotechnical Journal, **34**(6): 863–885. doi:10.1139/t97-055.

Price, W.A. 2009. Prediction manual for drainage chemistry from sulphidic geologic materials. Canadian MEND Report 1.20.1, dated December 2009. Natural Resources Canada.

Rayhani, M.T., Rowe, R.K., Brachman, R.W.I., Take, W.A., and Siemens, G. 2011. Factors affecting GCL hydration under isothermal conditions. Geotextiles and Geomembranes, **29**(6): 525–533. doi:10.1016/j.geotexmem.2011.06.001.

Rosin-Paumier, S., and Touze-Foltz, N. 2012. Hydraulic and chemical evolution of GCLs during filter press and oedopermeametric tests performed with real leachate. Geotextiles and Geomembranes, **33**: 15–24. doi:10.1016/j.geotexmem.2012.02.002.

Rosin-Paumier, S., Touze-Foltz, N., and Pantet, A. 2011. Impact of a synthetic leachate on permittivity of GCLs measured by filter press and oedopermeameter tests. Geotextiles and Geomembranes, **29**: 211–221. doi:10.1016/j.geotexmem.2010.11.001.

Rowe, R.K., and Abdelatty, K. 2012. Effect of a calcium-rich soil on the performance of an overlying GCL. Journal of Geotechnical and Geoenvironmental Engineering, **138**(4): 423–431. doi:10.1061/(ASCE)GT.1943-5606.0000614.

Rowe, R.K., and Hosney, M.S. 2013. Laboratory investigation of GCL performance for covering arsenic contaminated mine wastes. Geotextiles and Geomembranes, **39**: 63–77. doi:10.1016/j.geotexmem.2013.06.003.

Rowe, R.K., Quigley, R.M., Brachman, R.W.I., and Booker, J.R. 2004. Barrier systems for waste disposal facilities. Spon Press, London.

Rowe, R.K., Mukunoki, T., and Bathurst, R.J. 2006. Compatibility with jet A-1 of a GCL subjected to freeze-thaw cycles. Journal of Geotechnical and Geoenvironmental Engineering, **132**(12): 1526–1537. doi:10.1061/(ASCE)1090-0241(2006)132:12(1526).

Rowe, R.K., Mukunoki, T., and Bathurst, R.J. 2008. Hydraulic conductivity to Jet-A1 of GCLs after up to 100 freeze-thaw cycles. Géotechnique, **58**(6): 503–511. doi:10.1680/geot.2008.58.6.503.

Sari, K., and Chai, J. 2013. Self healing capacity of geosynthetic clay liners and influencing factors. Geotextiles and Geomembranes, **41**: 64–71. doi:10.1016/j.geotexmem.2013.08.006.

Scalia, J., and Benson, C. 2010a. Effect of permeant water on the hydraulic conductivity of exhumed GCLs. Geotechnical Testing Journal, **33**(3): 1–11.

Scalia, J., and Benson, C.H. 2010b. Preferential flow in geosynthetic clay liners exhumed from final covers with composite barriers. Canadian Geotechnical Journal, **47**(10): 1101–1111. doi:10.1139/T10-018.

Scalia, J., and Benson, C.H. 2011. Hydraulic conductivity of geosynthetic clay liners exhumed from landfill final covers with composite barriers. Journal of Geotechnical and Geoenvironmental Engineering, **137**(1): 1–13. doi:10.1061/(ASCE)GT.1943-5606.0000407.

Shackelford, C., Benson, C., Katsumi, T., Edil, T., and Lin, L. 2000. Evaluating the hydraulic conductivity of geosynthetic clay liners permeated with non-standard liquids. Geotextiles and Geomembranes, **18**: 133–162. doi:10.1016/S0266-1144(99)00024-2.

Shackelford, C., Sevick, G., and Eykholt, G. 2010. Hydraulic conductivity of geosynthetic clay liners to tailings impoundment solutions. Geotextiles and Geomembranes, **28**: 149–162. doi:10.1016/j.geotexmem.2009.10.005.

Shan, H., and Daniel, D. 1991. Results of laboratory tests on a geotextile/bentonite liner material. *In* Proceedings of the 91st Industrial Fabrics Association International Conference, St. Paul, Minn. pp. 517–535.

Wagner, J.F., and Schnatmeyer, C. 2002. Test field study of different cover sealing systems for industrial dumps and polluted sites. Applied Clay Science, **21**: 99–116. doi:10.1016/S0169-1317(01)00096-5.